A Nature Portfolio journal



https://doi.org/10.1038/s42003-025-08573-z

Profiling brain morphology for autism spectrum disorder with two cross-culture large-scale consortia

Check for updates

Xue-Ru Fan¹, Ye He², Yin-Shan Wang¹, Lei Li³, Lifespan Brain Chart Consortium (LBCC)*, China Autism Brain Imaging Consortium (CABIC)*, Xujun Duan ®³ ⋈ & Xi-Nian Zuo ®¹ ⋈

We explore neurodevelopmental heterogeneity in Autism Spectrum Disorder (ASD) through normative modeling of cross-cultural cohorts. By leveraging large-scale datasets from Autism Brain Imaging Data Exchange (ABIDE) and China Autism Brain Imaging Consortium (CABIC), our model identifies two ASD subgroups with distinct brain morphological abnormalities: subgroup "L" is characterized by generally smaller brain region volumes and higher rates of abnormality, while subgroup "H" exhibits larger volumes with less pronounced deviations in specific areas. Key areas, such as the isthmus cingulate and transverse temporal gyrus, were identified as critical for subgroup differentiation and ASD trait correlations. In subgroup H, the regional volume of the isthmus cingulate cortex showed a direct correlation with individuals' autistic mannerisms, potentially corresponding to its slower post-peak volumetric declines during development. These findings offer insights into the biological mechanisms underlying ASD and support the advancement of subgroup-driven precision clinical practices.

Autism Spectrum Disorder (ASD), or autism, is a lifelong neurodevelopmental condition characterized by impairments in social communication and the presence of repetitive, unusual sensory-motor behaviors^{1,2}. The global prevalence of ASD is approximately 1% in children³, with different rates reported in specific regions, such as 2.8% in children aged 8 years in the United States⁴ and 0.7% in children aged 6 to 12 years in China⁵. Several factors, including improved survey methodologies, diagnostic practices, public awareness and access to services, have contributed to this increase in prevalence^{3,6}. Over time, understanding of ASD has developed from a categorical diagnosis to a dimensional perspective of neurodiversity⁷. This change redefined autism as a spectrum that includes a wide range of characteristics within a unified framework8. However, the expanded diagnostic criteria may have too low thresholds for diagnosis9, and have introduced significant heterogeneity within ASD. This heterogeneity suggests that the term "spectrum" encompasses multiple subgroups with distinct etiological phenotypes10,11.

Recent neuroimaging studies increasingly highlight ASD's biological heterogeneity as a key barrier to identifying consistent brain-behavior relationships. Traditional case-control neuroimaging studies, which assume ASD and typical developing groups as homogeneous entities, often fail to

account for subgroup differences¹². This has led to inconsistent findings across brain regions and participants, further complicating efforts to identify reliable brain-behavior biomarkers. The decreasing effect sizes in group comparison studies over time 13 highlight the difficulty of constructing mechanistic models of ASD. This heterogeneity challenge extends to intervention research, where differential treatment responses across ASD subgroups^{14,15} suggest that precision approaches accounting for neurobiological variation could enhance outcomes. Data-driven clustering techniques have emerged as a promising approach to address this complexity by leveraging cognitive and behavioral profiles alongside patterns of brain morphology and function. Various clustering methods¹⁶⁻²⁰ have been used to identify meaningful subgroups, in order to uncover the neurobiological mechanisms of ASD and provide insights into subgroup-specific traits^{8,21}. While despite decades of effort, inconsistencies in sample selection, classification methods, and feature selection between studies remain significant challenges²¹. These issues have limited the ability of clustering techniques to consistently identify robust and replicable subgroups.

Inconsistencies in ASD studies may be due to altered neurodevelopmental adaptations²² and participant selection biases²³. These limitations highlight the need to group variables with strong biological relevance for the

¹State Key Laboratory of Cognitive Neuroscience and Learning, Faculty of Psychology, Beijing Normal University, Beijing, 100875, China. ²School of Artificial Intelligence, Beijing University of Posts and Telecommunications, Beijing, 100876, China. ³Sichuan Provincial Center for Mental Health, Sichuan Provincial People's Hospital, School of Life Science and Technology, University of Electronic Science and Technology of China, Chengdu, 610054, China. *Lists of authors and their affiliations appear at the end of the paper. ⊠e-mail: duanxujun@uestc.edu.cn; xinian.zuo@bnu.edu.cn

ASD subgroups²⁴. At the same time, individual differences in sex, intelligence, medication use, and comorbidities^{25,26}, along with methodological variability²⁷ in data acquisition and analysis, complicate the interpretation of the results of neuroimaging studies. In response to these challenges, normative modeling²⁸ techniques offer a promising framework to capture the full range of neurobiological variation¹². This approach enables standardized assessments by comparing an individual's brain morphology to population-based references²⁹. In previous ASD studies, references were often built on internal or public datasets^{18,20,30,31}, but the relatively small sample size limits the generalizability and reliability of the results. Recently, the Lifespan Brain Chart Consortium (LBCC, https://github.com/brainchart/lifespan) provided neurodevelopmental variations throughout life from the most inclusive data available³², providing a robust framework for us to achieve percentile-based comparisons of ASD with considerable statistical power.

This study adjusted the LBCC normative models in two large-scale cross-cultural ASD consortia: the China Autism Brain Imaging Consortium (CABIC, https://php.bdnilab.com)³³ and the Autism Brain Imaging Data Exchange (ABIDE, https://fcon_1000.projects.nitrc.org/indi/abide)^{34,35}. Focusing on childhood development, we used the largest-scale brain charts³² to explore neurodevelopmental heterogeneity in ASD before adolescence. We classified ASD into subgroups using spectral clustering based on Out-of-Sample (OoS) centile scores, a biological measure which quantified brain morphological deviations of ASD from normative growth. A Support Vector Machine (SVM) with Recursive Feature Elimination and Cross-Validation (RFECV) identified key brain regions driving subgroup classification. The ABIDE-based classifier was then applied to CABIC to identify similar subgroups. Brain-behavior analyses were performed separately for each dataset to identify reproducible subgroup-specific correlations. From a perspective of brain morphology, this work disentangles the mechanisms of mixed neurosubtypes and provides new insight into the biological complexity of ASD.

Results

Brain morphological profiles reveal two distinct autism subgroups

We first analyzed the ABIDE dataset. The distributions of the OoS centile scores across 34 bilateral Desikan-Killiany36 cortical volumes ranged from 0 to 1 (Supplementary Fig. 1a). OoS scores estimate the morphological variations of each participant in 34 brain regions compared to the median regional volumes of the population (50th centile, equivalent to a 0.5 OoS score). Relative to 0.5, individuals with more atypical phenotypes have more extreme scores. A Shapiro-Wilk test on the 34 OoS scores indicated that none followed a normal distribution (Table 1, column 2). Using spectral clustering on the OoS scores, we identified two distinct clusters (ASD subgroups) with the highest silhouette coefficient among cluster solutions ranging from two to ten (Fig. 1a). All p-values for between-subgroup comparisons (two-sample t-tests for the paracentral and pars orbitalis regions, and rank-sum tests for all other regions) were <0.001). One subgroup, referred to as "L", exhibited generally Lower OoS scores, while the other referred to as "H", displayed Higher scores (Table 1, columns 5 and 7).

Certain regions of the brain showed significant differences in their OoS score distributions between the two subgroups (Fig. 1g; Supplementary Fig. 1b. For CABIC results, please see Supplementary Fig. 2a and 2b). Subgroup H exhibited greater variability in the occipital lobe, particularly in the lingual gyrus, pericalcarine cortex, and cuneus. In contrast, subgroup L showed more pronounced reductions in these regions compared to the normative benchmark (0.5). Other regions, such as the pars opercularis and superior temporal gyrus, also exhibited subgroup-specific changes. The results of the Shapiro-Wilk test for OoS scores (Table 1, columns 4 and 6) indicated that more brain regions in subgroup H followed a normal distribution compared to subgroup L. Broader variability was observed in regions such as the entorhinal cortex in subgroup L and the pericalcarine in subgroup H, highlighting further subgroup-specific clustering.

Distinct structural and age differences between subgroups

The median OoS scores before clustering (Fig. 1b: Table 1, column 3) reveal a mixed pattern of deviations across regions. Most regions exhibit reduced volumes, particularly in the occipital lobe. However, some regions, such as the precuneus, paracentral lobule, transverse temporal gyrus, and insula, show slightly higher OoS scores. This combined pattern reflects overlapping structural deviations from both subgroup H and L (Fig. 1c), obscuring the distinct morphological differences that become evident after clustering. For instance, although subgroup L shows smaller volumes in the insula and precuneus, the larger volumes in subgroup H predominantly drive the combined pattern in the whole population. In contrast, smaller volumes of the lingual gyrus and the middle temporal gyrus in subgroup L have a stronger influence on the overall result. Some regions, such as the pericalcarine cortex, are almost entirely influenced by subgroup L. Meanwhile, regions like the inferior and superior temporal gyrus exhibit volumes close to the normative average because of the contrasting characteristics of both subgroups effectively canceling each other out.

To identify the brain regions most associated with morphological abnormalities, we calculated the prevalence of abnormalities for each region in the two subgroups. The prevalence represents the percentage of participants with OoS scores below 0.025 (2.5% centile) for subgroup L, while above 0.975 (97.5% centile) for subgroup H. Subgroup L (Fig. 1f; Table 1, column 8) exhibited the highest prevalence of abnormalities in regions such as the middle and inferior temporal gyrus, pericalcarine cortex, frontal pole, and medial orbital frontal gyrus. In contrast, subgroup H (Fig. 1f; Table 1, column 9) generally exhibited less severe abnormalities, with a concentration in the insula, transverse temporal gyrus, and caudal anterior cingulate. Participants in subgroup L were significantly younger than those in subgroup H (Fig. 1h; p = 0.02, Supplementary Table 1). However, no significant differences were observed in the category PDD (p = 0.32), the MRI scanner model (p = 0.07) and the manufacturer (p = 0.86), the data collection site (p = 0.16) (Fig. 1k), IQ (Fig. 1i, see Supplementary Table 1 for details), or scores from ADI-R (Fig. 1j), SRS (Fig. 1l), and ADOS-2 (Fig. 1m). The corresponding results for CABIC are shown in Supplementary Fig. 3.

Machine learning reveals subgroup morphological features

The optimized SVM model for the identification of subgroups demonstrated robust predictive performance. It used a polynomial kernel with a regularization parameter C=0.1 and a kernel coefficient $\gamma=1$. The model achieved a high classification accuracy (0.95, p<0.001) and a F1 score (0.94, p<0.001) in five cross-validation folds. Figure 1d shows the SHapley Additive exPlanations (SHAP) summary plot for the top 10 selected features. Figure 1e and Supplementary Table 2 summarize the mean SHAP values for all 29 selected regions. SHAP values 37 quantify the contribution of individual brain regions to the predictions of the model. Among the regions, the isthmus cingulate, entorhinal cortex, precuneus, and middle temporal gyrus emerged as the most predictive features. Higher SHAP values for these regions were strongly associated with subgroup H, while lower values corresponded to subgroup L. These findings indicate different volumetric patterns in the cingulate, temporal, and parietal areas, effectively distinguishing the two subgroups.

Distinct structural covariance patterns across subgroups

Structural covariance analysis on OoS scores revealed significant correlations between brain regions, with distinct patterns observed across ASD subgroups and control group (Fig. 2c). These patterns were reproduced in both the ABIDE and CABIC datasets. In subgroup H, enhanced covariation was identified between the isthmus cingulate and the caudal middle frontal region (ABIDE: z=2.88, p=0.00; CABIC: z=2.25, p=0.02). In subgroup L, the parahippocampal gyrus showed reduced covariation with the entorhinal cortex (ABIDE: z=-2.07, p=0.04; CABIC: z=-3.25, p=0.00). Similarly, reduced covariation was observed between the posterior cingulate and the entorhinal cortex (ABIDE: z=-2.64, p=0.01) and between the insula and the entorhinal cortex (ABIDE: z=-3.30, p=0.00; CABIC: z=-2.8, p=0.03). An increased covariation was

Table 1 | Group comparisons of regions morphology between overall and two ASD subgroups

Region	OoS Scores						AbP¹(%)	
	All		L		Н		L	Н
	p	Median	p	Median	p	Median		
Superior frontal	0.01	0.48	0.02	0.28	0.37	0.62	5.56	2.70
Rostral middle frontal	0.01	0.46	0.02	0.25	0.32	0.60	7.94	0.68
Caudal middle frontal	0.00	0.42	0.00	0.26	0.05	0.60	6.35	2.70
Pars opercularis	0.00	0.47	0.00	0.23	0.07	0.61	6.35	4.73
Pars triangularis	0.00	0.45	0.02	0.28	0.02	0.60	6.35	1.35
Pars orbitalis	0.01	0.46	0.06	0.33	0.11	0.56	5.56	0.68
Frontal pole	0.00	0.48	0.02	0.34	0.03	0.60	11.90	2.03
Lateral orbital frontal	0.00	0.46	0.01	0.26	0.06	0.63	7.94	2.03
Medial orbital frontal	0.00	0.42	0.00	0.26	0.04	0.61	10.32	2.70
Rostral anterior cingulate	0.00	0.45	0.00	0.25	0.04	0.65	4.76	2.70
Caudal anterior cingulate	0.00	0.47	0.01	0.30	0.00	0.68	3.97	6.76
Precentral	0.00	0.45	0.01	0.26	0.17	0.60	6.35	3.38
Paracentral	0.01	0.52	0.05	0.34	0.10	0.62	4.76	5.41
Postcentral	0.00	0.48	0.01	0.29	0.05	0.64	7.14	4.05
Supramarginal	0.00	0.49	0.01	0.31	0.04	0.65	7.94	3.38
Posterior cingulate	0.00	0.46	0.02	0.29	0.04	0.64	7.94	5.41
Isthmus cingulate	0.00	0.47	0.00	0.27	0.06	0.64	3.97	4.05
Precuneus	0.00	0.52	0.04	0.29	0.02	0.70	5.56	4.73
Superior parietal	0.00	0.44	0.00	0.27	0.08	0.60	7.94	2.70
Inferior parietal	0.00	0.45	0.07	0.30	0.02	0.63	7.94	2.03
Transverse temporal	0.00	0.52	0.02	0.32	0.03	0.68	7.94	6.08
Banks superior temporal	0.00	0.44	0.00	0.26	0.02	0.59	3.97	5.41
Superior temporal	0.00	0.49	0.00	0.26	0.04	0.67	6.35	4.05
Middle temporal	0.00	0.44	0.02	0.24	0.06	0.61	17.46	2.70
Inferior temporal	0.00	0.49	0.05	0.30	0.04	0.62	11.90	0.68
Fusiform	0.00	0.45	0.01	0.26	0.09	0.59	10.32	1.35
Parahippocampal	0.00	0.49	0.02	0.33	0.01	0.63	3.17	2.70
Entorhinal	0.01	0.51	0.05	0.40	0.04	0.62	6.35	0.68
Temporal pole	0.00	0.44	0.03	0.36	0.02	0.58	10.32	1.35
Lateral occipital	0.00	0.46	0.01	0.28	0.02	0.63	9.52	2.70
Lingual	0.00	0.40	0.00	0.24	0.01	0.58	7.94	2.70
Pericalcarine	0.00	0.36	0.00	0.23	0.01	0.53	11.90	2.70
Cuneus	0.00	0.46	0.01	0.25	0.03	0.55	6.35	1.35
Insula	0.00	0.53	0.02	0.31	0.02	0.69	3.17	6.08
		-					-	

¹AbP Prevalence of abnormalities.

observed in subgroup L between the parahippocampal gyrus and the lateral occipital cortex (ABIDE: z = 1.97, p = 0.05; CABIC: z = 2.04, p = 0.04).

Brain-behavior correlations in Subgroup H

We examined correlations between cortical region volumes (OoS scores) and clinical measures in the ABIDE and CABIC datasets, identifying significant associations that were consistent between both datasets. All significant correlations were found within subgroup H. The transverse temporal gyrus showed positive correlations with ADOS (ADOS-2 in ABIDE and ADOS in CABIC) Total and Social Affect scores (Fig. 2a). In the CABIC dataset, moderate correlations were observed for Total (r(198) = 0.17, p = 0.02) and Social Affect (r(191) = 0.21, p = 0.00) score. Stronger correlations were identified in the ABIDE dataset for Total (r(93) = 0.24, p = 0.01) and Social Affect (r(93) = 0.20, p = 0.04) score. The inferior temporal gyrus was positively correlated with RRB (restricted interests and repetitive behaviors), with a slightly stronger correlation in

ABIDE (r(94) = 0.19, p = 0.05) compared to CABIC (r(189) = 0.17, p = 0.02). The volumetric centile of the isthmus cingulate is correlated with SRS Autistic Mannerisms, showing a higher correlation in ABIDE (r(58) = 0.33, p = 0.01) than in CABIC (r(192) = 0.14, p = 0.04). No significant correlations were identified between structural covariance patterns and cognitive behavior outcomes.

As a common comorbidity of ASD, intellectual disability is closely associated with atypical brain morphological developmental patterns that accompany individual differences in intellectual functioning. To examine whether Full-Scale Intelligence Quotient (FIQ) mediates the relationships between brain morphology and cognitive behaviors within clusters, mediation analyses were conducted on the significant correlations we found in subgroup H. Results revealed direct effects for specific cortical regions (Fig. 2b). The transverse temporal gyrus showed a direct effect on ADOS-2 Total (C' = 0.21, p = 0.03), while the isthmus cingulate exhibited a direct effect on SRS Autistic Mannerisms

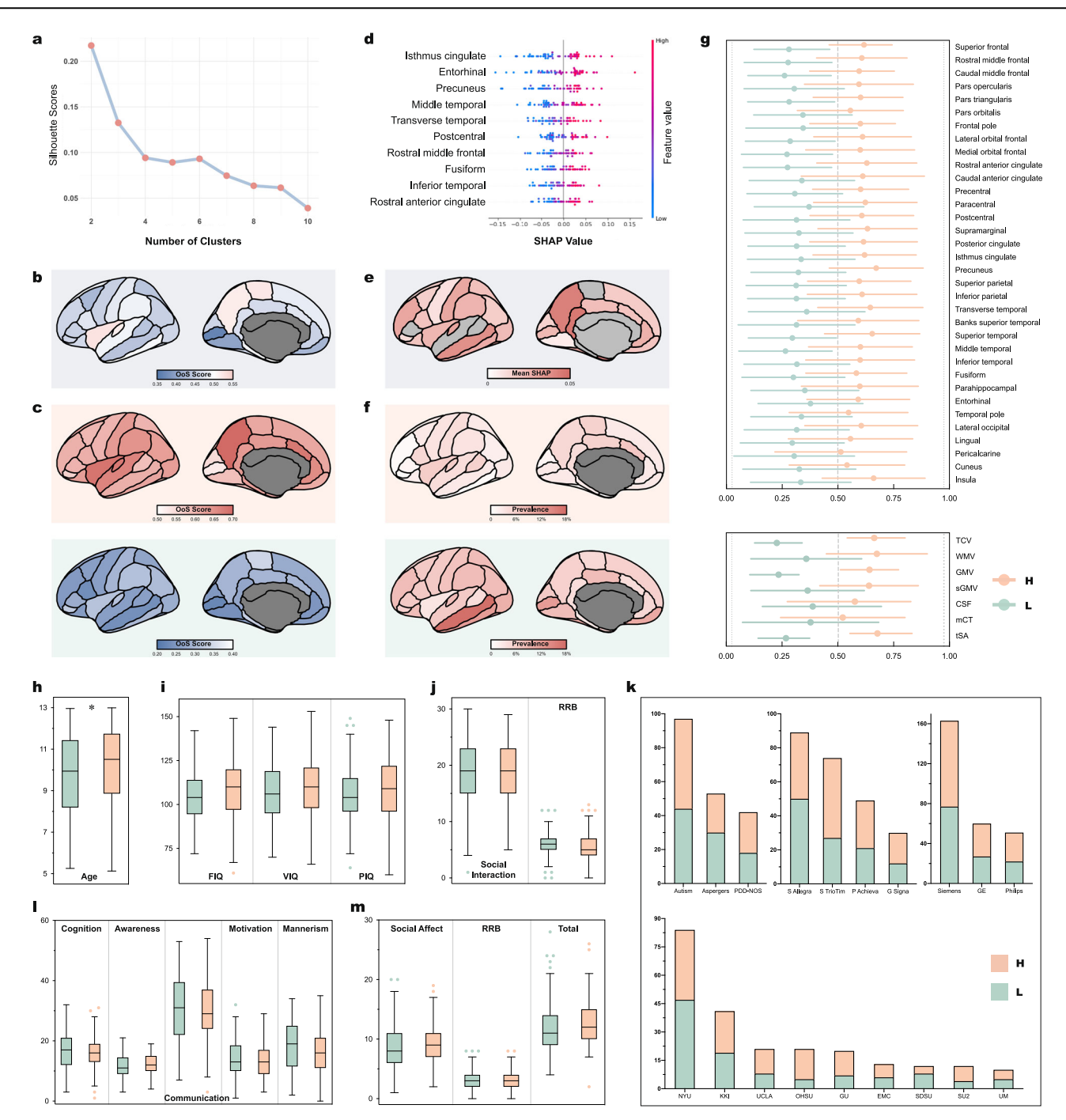


Fig. 1 | Clustering-derived subgroups reveal distinct brain morphological patterns in ASD from ABIDE dataset. a Silhouette scores across different clustering solutions (2 to 10 clusters). The highest silhouette score indicates two distinct subgroups. b Median OoS scores of 34 cortical regions before clustering. c Median OoS scores of ASD subgroup H (top) and L (bottom). d SHAP summary plot displaying the top 10 brain regions with the highest contributions to the SVM model's predictions. e The mean SHAP values across the 29 selected cortical regions contributed to the classification. f Prevalence maps depicting the proportion of participants with extreme (2.5% for subgroup L, 97.5% for subgroup H) structural anomalies. g OoS scores across 34 cortical regions (top) and global measures (bottom) for subgroup H (orange) and L (green). TCV total cortical volume, WMV total white matter volume, GMV total cortical gray matter volume, sGMV total

subcortical gray matter volume, CSF total ventricular cerebrospinal fluid volume, mCT mean cortical thickness, tSA total surface area, Dots indicate the mean value of OoS scores, bars indicate the standard deviation. See Supplementary Information Supplementary Fig. 1b and Supplementary Fig. 1d for detailed density plots. Distribution of participant ages (\mathbf{h}); IQ scales (\mathbf{i}); ADI-R (\mathbf{j}); PDD category (\mathbf{k} , top left), MRI scanner model (\mathbf{k} , top middle), manufacturer (\mathbf{k} , top right), and data collection site (\mathbf{k} , bottom); SRS (I); and ADOS (\mathbf{m}) across the two subgroups, with subgroup L participants being significantly younger than those in subgroup H (p=0.02). Note, the left hemispheres are plotted in (\mathbf{b} , \mathbf{c} , \mathbf{e} , and \mathbf{f}) just for visualization purposes. For plots \mathbf{h} – \mathbf{j} , \mathbf{l} , and \mathbf{m} , the center line shows the median; the box limits represent the 25th and 75th percentiles; the whiskers show the minimum and maximum values; and the dots represent potential outliers.

(C' = 0.32, p = 0.01). As our analysis relied on cross-sectional data, the observed brain-behavior relationships represent correlations rather than causal effects. Our mediation hypotheses regarding developmental brain-behavior causality require validation through longitudinal studies.

While no mediation effects through FIQ were observed, both from brain → cognitive behaviors or in reverse (Supplementary Fig. 4). Neither direct nor indirect effects were significant for correlations to ADOS-2 RRB or Social Affect.

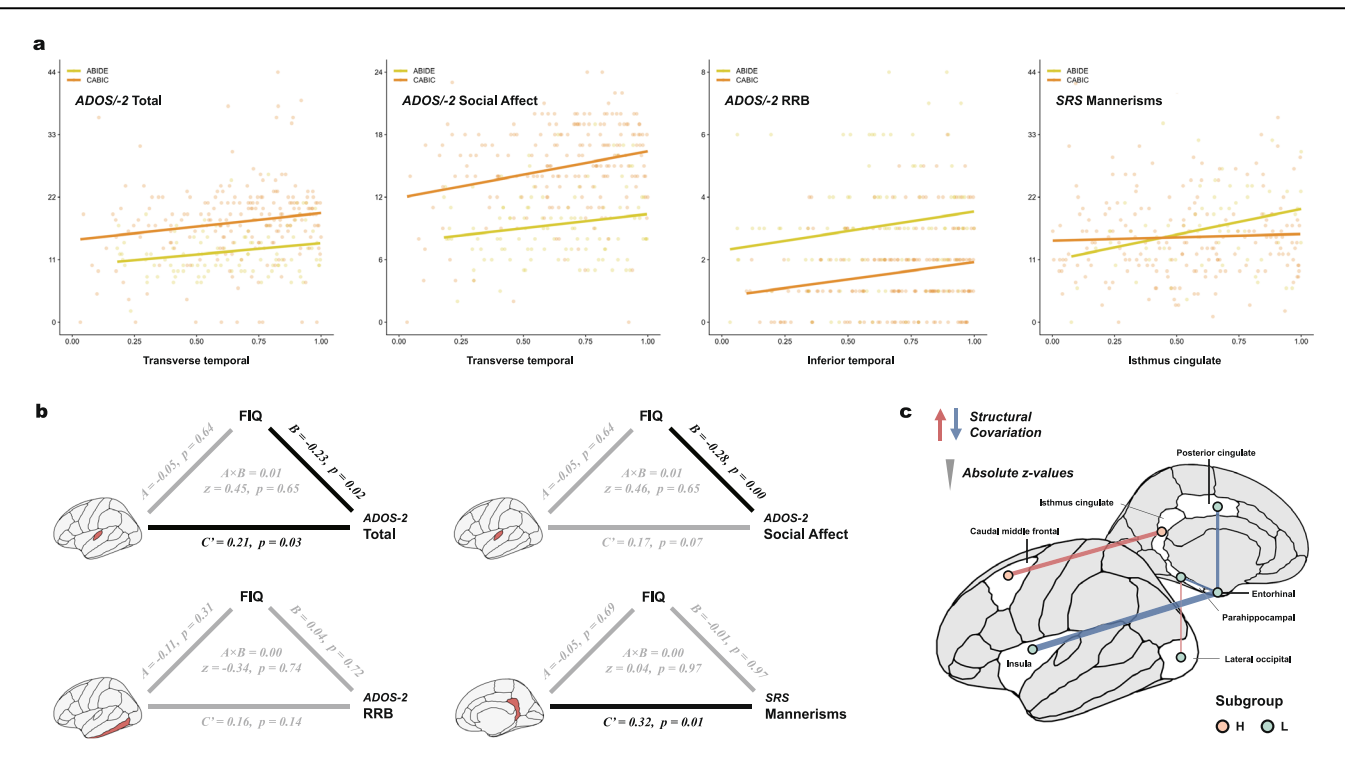


Fig. 2 | Brain-behavior correlations and structural covariations of Out-of-Sample scores. a Reproducible correlations between brain region volumes, measured as Out-of-Sample (OoS) scores, and clinical measures across ABIDE and CABIC datasets (subgroup H only). b Mediation models for significant brain-behavior associations identified in subgroup H (ABIDE cohort only). Black solid arrows represent

significant effects, while gray arrows indicate non-significant ones. Top: transverse temporal; bottom left: inferior temporal; bottom right: isthmus cingulate. c Significant structural covariations across ABIDE and CABIC datasets. Positive *z*-values (red lines) indicate stronger covariance in ASD participants compared to controls, while negative *z*-values (blue lines) reflect weaker covariance.

Discussion

This study used the ABIDE and CABIC datasets to discover distinct brain morphological subgroups of ASD within a young male cohort. We identified two subgroups characterized by significant differences in OoS scores in 34 cortical regions. Machine learning models showed a high predictive accuracy in distinguishing these subgroups based on their brain morphology. Furthermore, structural covariance and brain behavior correlation analysis illustrated different patterns of morphological relationships and their associations with clinical measures, especially in subgroup H. The consistent correlations across both the ABIDE and CABIC datasets highlight the robustness and reproducibility of our results across diverse cohorts. We will now discuss these findings from several neurobiological and neurodevelopmental perspectives to enhance our understanding of the distinct morphological patterns identified.

Studies have reported extremely large or small head circumferences in individuals with ASD, possibly related to different subgroups. Early brain overgrowth is one of the most consistent findings in ASD research³⁸. Abnormal increases in brain size during early development suggest that atypical cell proliferation significantly contributes to ASD symptoms³⁹. Ultrasound studies have detected head enlargement during the second trimester in individuals later diagnosed with ASD⁴⁰. iPSC-based studies reveal enlarged embryonic stage brain cortical organoids (BCOs) in babies with ASD, with larger BCOs associated with more severe social symptoms⁴¹. MRI scans of these individuals show overgrowth in primary auditory and somatosensory cortices, while undergrowth in the visual cortex⁴¹. This neuronal overproduction, caused by the acceleration of the cell cycle, results in impaired differentiation and ultimately disrupts neural functions⁴².

Smaller brain volumes are also frequently reported in ASD. A metaanalysis⁴³ identified volumetric reductions in a large cluster of regions, including the parahippocampal gyrus and entorhinal cortex. Higher levels of autistic traits have been associated with a smaller total cortical volume (TCV), a lower cortical thickness, a smaller surface area and a lower gyrification^{44,45}. One potential explanation for this global brain underdevelopment is impairment caused by insufficient blood circulation and oxygen saturation⁴⁶. For example, children with complex congenital heart disease (CHD) also demonstrate cognitive difficulties similar to those observed in ASD and have an increased likelihood of developing ASD⁴⁷. Similarly, head enlargement also coincide with greater increases in height often⁴⁵. Therefore, brain overgrowth could be part of the broader physical growth dysregulation⁴⁸ too.

These evidences provide the distinct neurobiological basis for the subgroups identified in our study. The different underlying physiological mechanisms may explain the inconsistent effectiveness of commonly used pharmacological treatments. For example, unsupervised data-driven cluster analysis on ASD children revealed an optimum of two intranasal oxytocin intervention-sensitive subtypes⁴⁹. Our discovery of two distinct ASD subtypes with divergent brain morphologies further supports the necessity for subtype-specific therapeutic strategies. Future research focusing on targeted pharmacological interventions for individual subtypes will not only explain how these treatments modulate brain function and ultimately translate into clinical benefits, but also advance personalized medicine in ASD. Specifically, by mapping neurobiological heterogeneity to differential therapeutic outcomes, this approach could reconcile previous inconsistencies in treatment efficacy while optimizing intervention protocols for mechanistically defined patient subgroups.

Abnormal neural migration and cortical laminar organization in ASD⁵⁰ suggest that structural abnormalities are unlikely to be localized. Postmortem studies have identified focal laminar disorganization and mis-migrated neurons in the prefrontal and temporal cortex, particularly in layers 2, 3, and 4^{50} . Layers 2 and 3 support information exchange between cortical regions, while layer 4 receives sensory inputs⁵¹. Disruptions in these layers can cause profound miscommunication between the sensory and higher-order cognitive regions. Key regions in our clustering analysis (such as the precuneus, isthmus cingulate, and entorhinal cortex; Fig. 3a, $a\sim c$) are primarily involved in higher-order association networks (Fig. 3a). As an idea for exploring hierarchical

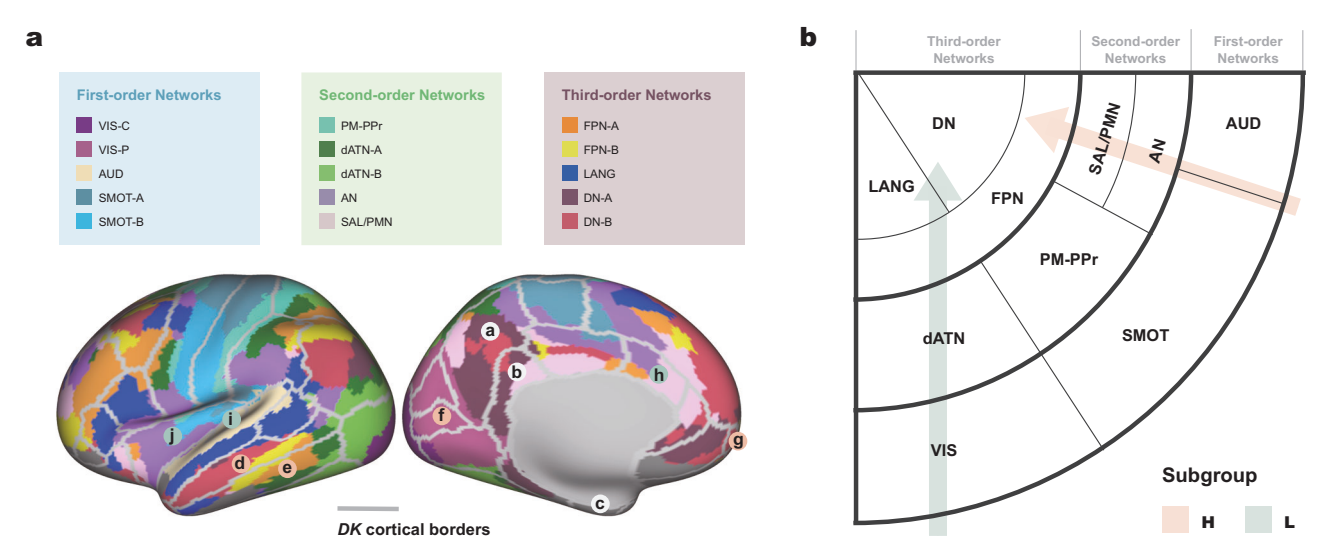


Fig. 3 | The theoretical brain functional network impairment model of two ASD subgroups. a A brain map combining the 34 Desikan regions³⁶ with the latest 15 large-scale brain functional networks estimated from individuals⁵⁷. a, precuneus; b, isthmus cingulate; c, entorhinal; d, middle temporal; e, inferior temporal gyrus; f, pericalcarine; g, frontal pole; h, caudal anterior cingulate; i, transverse temporal; and i, insula. b A schematic of the potential spatial distributions of distinct functional

impairment networks inferred from 34 cortical regions with high abnormal prevalence for two subgroups. VIS Visual (C Central, P Peripheral), SMOT Somatomotor, AUD Auditory, dATN Dorsal Attention, PM-PPr Premotor-Posterior Parietal Rostral, AN Action-mode network, SAL/PMN Salience/Parietal Memory Network, FPN Frontoparietal Network, LANG Language, DN Default-mode Network.

information flow of functional connectivity, Stepwise Functional Connectivity (SFC) analysis was introduced to disentangle brain functional networks, and has discovered the complex connectivity transitions from primary sensation to higher-order association regions of the brain 52,53. These existing information flow suggest different pathways of impairment as the basis for the heterogeneity of ASD. Inconsistencies in information flow reported by previous ASD studies 21,54 may arise from two distinct structural impairment patterns identified in our study.

The regional volume abnormalities identified in our study involve distinct functional brain regions in the two subgroups. Subgroup L showed a notable prevalence in the middle temporal gyrus, inferior temporal gyrus, pericalcarine cortex and frontal pole (Fig. 3a, $d\sim g$), while subgroup H in the caudal anterior cingulate, transverse temporal cortex, and insula (Fig. 3a, $h\sim 1$). Drawing on the spatial distributions⁵⁵ of 7 large-scale functional networks⁵⁶, we constructed a schematic (Fig. 3b) of the latest 15 large-scale functional networks of the brain estimated from individuals⁵⁷ (Fig. 3a). This perspective revealed different pathways of functional impairment in the regions with a high prevalence of abnormalities for each subgroup. Subgroup L exhibited an atypical morphology mainly affecting Visual - Dorsal Attention - Frontoparietal - Language and Default-mode networks (Fig. 3b, green path), while subgroup H affected the Auditory and Somatomotor -Action-mode and Salience/Parietal Memory - Frontoparietal networks (Fig. 3b, orange path), indicating disturbances in peculiar unimodal sensory integration and multimodal cortical functions. These networks are organized by three-order hierarchy that are agree well with myelination reference maps⁵⁷, showing that the cerebral cortex develops sequentially, radiating outward from motor and sensory cortex⁵⁸.

This phenomenon may hint at the presence of distinct abnormal brain functional circuits from first- to third-order networks in the subgroups. For example, in adults without ASD⁵⁹, increased gray matter volume in regions of the somatomotor network was associated with greater attention to detail, while changes in regions of the visual network were associated with poor imagination. These findings suggest potential cognitive patterns in two subgroups of ASD that have yet to be discovered. At the same time, these two subgroups we found may respond differently to biologically targeted therapies, emphasizing the need for more personalized approaches. For example, functional connectivity-guided continuous theta-burst stimulation (cTBS) on individual's dorsolateral prefrontal cortex target with the strongest connectivity to amygdala significantly improve social

communication skills in minimally verbal ASD children⁶⁰. As a reduction in brain volume and improvements in behavior outcomes, this ASD subtype likely fit the characteristics of subgroup H in our study. Targeted modulation of subgroup specific impairment pathway may gain better therapeutic effects, therefore further refine treatment protocols for better translational outcomes. In this case, if observed social improvements stem from rebalancing the subgroup H pathway, future interventions could achieve enhanced treatment efficacy by employing personalized neuromodulation protocols that precisely target the most morphologically burdened brain regions within this circuitry.

In typically developing children, the principal functional gradient⁵⁵ of the cortical organization reflects differentiation within unimodal sensory areas, progressing from the somatomotor and auditory cortex to the visual cortex. The transition from childhood to adolescence extends this organization to higher-order association cortices⁶¹. Brain maturation appears to involve a shift from local to distributed network architecture. The distinct morphological abnormalities in these two ASD subgroups, observed before this transition begins, raise a critical question: How do these "morphological foundations" disrupt their development from childhood to adolescence? These structural impairment pathways in childhood are likely to contribute further to heterogeneity in ASD during and after adolescence.

Different network-based vulnerabilities suggest that interventions targeting specific impairments within each subgroup could be more effective. Interestingly, we found no significant differences in cognitive or behavioral measures between the subgroups. Although there distinct patterns of structural covariation between subgroups, but no significant correlations with autism-related behaviors. Structural covariance reflects long-term developmental changes. Reduced structural covariance may indicate disruptions in shared developmental pathways, while enhanced covariance could result from compensatory adaptations in response to atypical neurodevelopmental trajectories in ASD. This implies that morphological deficiencies may activate compensatory mechanisms during development, leading to similar cognitive and behavioral outcomes.

These neurodevelopmental compensation mechanisms raise questions about the stability of subgroup morphology distinctions across different developmental stages. To validate the robustness of our ASD clusters across different development stage, we implemented sliding 4-year age windows (with a predefined threshold of at least 80 participants to ensure statistical power). For each window, we applied the identical spectral clustering

pipeline and evaluated the consistent cluster indices across each narrow age range and the full age range. All the narrow age range population yielded two distinct brain subtypes as similar as the characteristics in our main results. The assignment consistency were 90.48% (5–8.9 yrs, N = 84), 91.89% (6–9.9 yrs, N = 111), 98.67% (7–10.9 yrs, N = 150), 97.71% (8~11.9 yrs, N = 175) and 88.42% (9~12.9 yrs, N = 190). These remarkable consistency in subgroup classification suggests that the specific impairments on brain morphology are consistently maintained across development.

The observed age difference between subgroups, though minor, could have significant implications during sensitive developmental periods. Lifespan trajectories³² of 34 brain regions show an early steep increase in volume, followed by a near-linear decline. The middle temporal gyrus peaks at 7.8 years, while the caudal anterior cingulate peaks at 9.2 years³², possibly related to the result that subgroup L is generally younger than subgroup H. However, in the CABIC cohort, we observed an inverse age relationship across both classification methods (whether using the ABIDE-classifier or independent clustering), with the subgroup L being significantly older than the H (Supplementary Fig. 3a and 5i). The age difference subgroups needs future studies with larger sample sizes to validate. While here, we propose some possible reasons for the ABIDE cohort to understand that these distinct structural abnormalities likely reflect differences in the timing of atypical developmental processes.

The isthmus cingulate, a key region in subgroup clustering, typically peaks in volume at 3.8 years. The lack of age-related decline in cortical volume was consistently found in subgroup H in both the ABIDE and CABIC datasets (See Supplementary Analysis and Supplementary Fig. 1f). However, subgroup H aligns with normative references before age 5, while subgroup L shows smaller initial volumes (Supplementary Fig. 1e). In subgroup H, an increase in structural covariance between the caudal middle frontal cortex (peaking at 7.75 years) and the isthmus cingulate (Fig. 2c) suggests synchronized developmental trajectories. This may reflect precocious caudal middle frontal development, delayed isthmus cingulate development, or both regions following similarly abnormal patterns²². Correlation analyses link larger isthmus cingulate volumes in subgroup H directly with more pronounced autistic mannerisms (Fig. 2a). These evidence hint at delayed development of the isthmus cingulate in subgroup H. With a normal OoS distribution (p = 0.06; Table 1, column 6) in this subgroup, this morphological change appears to represent a homogeneous and quantifiable pattern. In subgroup L, the parahippocampal gyrus (peaking at 10.63 years) shows reduced covariance with the entorhinal cortex (peaking at 22.67 years) but increased covariance with the lateral occipital cortex (peaking at 5.21 years). This pattern suggests a precocious development of the parahippocampal gyrus and/or the delayed lateral occipital cortex in this subgroup. Enhanced structural covariances may also reflect compensatory adaptations to mitigate structural disadvantages inherent in abnormal developmental patterns.

Recent genome-wide association studies (GWAS)⁶² reveal that cortical phenotypes exhibit distinct genetic architectures, with shared genetic variants influencing both normative brain size variation. Furthermore, significant genetic correlations between cortical expansion patterns and cognitive measures suggest multi-level mechanisms underlying neurodevelopment. These findings collectively motivate future study of ASD to build longitudinal cohorts to explore how genetically mediated cortical maturation trajectories influences different stages of development in ASD subgroups. Such approaches would bridge genotype-phenotype mapping to clinically biomarkers, advancing precision diagnostics and targeted interventions during sensitive neurodevelopmental windows.

One key contribution of this study is the reproducibility of brainbehavior associations across the ABIDE and CABIC datasets. In our analysis, we didn't apply on any multiple comparisons correction, three considerations may explain. First, the dual-dataset cross-validation design required consistent results across two independent cohorts (heterogeneous in culture/age), which substantially reduces false-positive risks through empirical replication. Second, as this is an exploratory target-discovery studies, overly conservative adjustments might obscure biologically meaningful results. Third, the cross-population reproducibility were prioritized in our study. We considered that uncorrected-but-replicated results had greater biological credibility than findings that were statistically corrected but failed to replicate. As a result, this cross-dataset validation confirms that the findings reflect stable neurobiological characteristics.

In subgroup H, an enlarged transverse temporal gyrus may impair precise auditory processing. This disruption can affect auditory responsiveness and the ability to integrate and understand information during social interactions. It may also damage early language perception and acquisition, particularly before a diagnosis of ASD is made. Research has found that when ASD is accompanied by cognitive learning needs, head enlargement becomes even more pronounced⁴⁵. This suggests a shared mechanism linking brain overgrowth with impaired intellectual functioning. Alternatively, cognitive impairments might mediate the relationship between this overgrowth and ASD. Although intelligence moderates the relationship between ASD traits, transverse temporal gyrus abnormality remains a direct indicator (Fig. 2b). This suggests impaired primary sensory perceptual function that is directly disrupted by abnormal sensory input. The inferior temporal gyrus (ITG) is also uniquely associated with restricted interests and repetitive behaviors, despite the low prevalence of structural abnormalities in subgroup H. This region plays a crucial role in object recognition⁶³. Disruptions in these functions can lead to a tendency to focus repetitively on objects or details. While as the RRB scale in ADOS cannot depict all the dimensions of repetitive behaviors, related results need future studies focusing on more detailed investigations on RRB to validate.

We classified ASD subtypes solely based on brain morphology, assuming a causal relationship between brain structure and cognition. However, this relationship is inherently complex, thus interpreting the brain in regions goes against its interconnected nature. Although subgroup L exhibited a higher prevalence of structural abnormalities, suggesting more extensive morphological variations, we did not find reproducible brainbehavior associations between cohorts. Several factors may explain these findings. First, cognitive impairments related to structural abnormalities in subgroup L might be more sensitive to cultural differences. Second, the validity of ASD diagnoses in subgroup L might be questionable. The best predictor of a DSM-IV diagnosis has been found to be often the specific clinic attended, rather than any defining characteristic of the individual⁶⁴. This indicates that current diagnostic tools may not capture the nuanced behaviors directly related to brain abnormalities in subgroup L. Considering global reduction in brain volume, which may result from cardiogenic etiological damage, our findings highlight the urgent need for new methods and paradigms to enable deep phenotyping and reduce the reliance on behavioral scales for differentiation. Third, heterogeneity within subgroups may also contribute to the limited reproducibility findings. Behavioral paradigms targeting brain regions with a normal distribution of OoS scores could better reveal subgroup-specific relationships between brain morphology and cognitive behavior.

In our analysis, we have rigorously controlled for site effects to minimize their impact on the results. To validate our approach, we performed independent spectral cluster analysis using only NYU site data from ABIDE. The assignment consistency compare with the main analysis reached 90.48%, demonstrating both the robustness of our clustering framework to site-specific variability and the biological validity of the identified subtypes. This high concordance further supports the clinical translatability of our neurosubtyping scheme, as it exists even when derived from diverse data sources, therefore providing a solid foundation for future multi-site biomarker development targeting subtype-specific mechanisms.

Some limitations in this study should be noted. First, previous research highlights atypical structural connectome asymmetry in ASD⁶⁵, while we could not fully evaluate hemispheric differences within subgroups using LBCC trajectories. Second, the cross-sectional nature of the data limits causal inferences about how these abnormalities of the brain morphology arise and their relationships with ASD symptoms. Future research should thoroughly investigate brain function and cognitive differences between these subgroups while exploring how demographic, environmental, and

developmental factors shape brain-based subtypes. Combining longitudinal data in vivo and in vitro 42 could expand cohort diversity and provide deeper insights into the neurobiological and molecular mechanisms underlying different subtypes. When designing research cohorts to study further, focus on more representative ASD prototypes 66 could help reduce heterogeneity within subgroups. Third, we should note that the use of ADOS rather than ADOS-2 in the CABIC cohort represents a methodological limitation that future studies with larger datasets should address.

More attention should be paid on people with more severe ASDs, such as minimally verbal autism, who remain underrepresented in brain imaging studies⁶⁷, partly due to the challenges of collecting neuroimaging data, especially in young children. Our research strategy uses structural magnetic resonance imaging, feasible in natural sleep or sedation, with significant clinical potential. However, multimodal approaches with higher ecological validity are essential to identify neurosubtypes that include these samples. Importantly, all current findings are derived from male ASD cohorts, any clinical translations should be cautiously limited to male populations until validated in females. Therefore, future studies should expand ASD cohorts with more female representation to enable comprehensive study of sexspecific brain morphological heterogeneity.

At the same time, replication with different clustering algorithms is required to confirm the stability of these findings. For example, we employed Gaussian mixture modeling (GMM) as a validation framework to assess consistency with our main clustering results. GMM assumes the observed data are generated from a mixture of multiple distinct Gaussian distributions⁶⁸. As the high cluster indices consistency (83.58%) across both methods, the brain morphology and cognitive behavior have the similar characteristics as spectral clustering analysis (Supplementary Fig. 6). Participants in subgroup L were also significantly younger than those in subgroup H (p = 0.03). No significant differences were observed in other comparisons between two subgroups. These replication with GMM demonstrates that our ASD neurosubtyping is not method-dependent. While more nuanced clustering approaches and strategies should be explored in the future, as disease variations may exist within the range of normal variation⁶⁹, and multiple subpopulations may also exist in typically developing populations⁷⁰. Finally, translational studies using animal models are essential for understanding the mechanisms underlying these different subtypes. Such studies can provide critical information on how abnormalities in brain morphology develop⁷¹.

Conclusion

Linking specific brain morphology abnormalities to cognitive or behavioral impairments in ASD is challenging. Different biological mechanisms can lead to similar behavioral outcomes, complicating the identification of neural correlates. This overlap may explain the difficulty in replicating neuroimaging findings between studies or cohorts. Using the largest brain normative datasets and two large-scale cross-cultural consortiums, we applied normative modeling to disentangle the heterogeneity of brain morphology in ASD. By breaking the ASD population into smaller and more morphologically homogeneous subgroups, we identified two subtypes of morphological abnormalities. We identified significant correlations between cortical regions and autistic traits across both consortia, with particular emphasis on the isthmus cingulate cortex, as well as the transverse and inferior temporal gyri. Based on the abnormal prevalence of regional volumes, we found two structural impairment pathways that could disrupt sensory to higher cognitive functions. These findings highlight the importance of untangling mixed biological mechanisms and offer insight to develop effective subgroupdriven individualized interventions. In conclusion, our study provides a reference for elucidating the etiological mechanisms of neurodevelopmental disorders and advancing future subgroup-driven precision clinical practice.

Methods

Participants and data preprocessing

Participants were selected from the Autism Brain Imaging Data Exchange cohort^{34,35}. The original dataset includes 1060 autistic and 1166 non-autistic

individuals aged 5~64 years from 24 different sites. All diagnoses were based on the DSM-IV or DSM-V criteria. We used T1-weighted MRI data from the ABIDE (I and II) cohort. The acquisition parameters are publicly available at https://fcon_1000.projects.nitrc.org/indi/abide/. Data quality was assessed through manual visual inspection aided by visualization outputs from *MRIQC* (https://mriqc.readthedocs.io/en/latest/)⁷² (version 22.0.6). We visually rated the quality of 2451 images using a 3-class framework⁷³, with "0" denoting images that suffered from gross artifacts and were considered unusable, "1" with some artifacts, but that were still considered usable, and "2" free from visible artifacts. Images with an "0" score (for example, with severe motion artifacts, segmentation errors, or structural abnormalities) were excluded. A total of 1907 (77.8%) images from 1726 participants passed the quality control. For the participants who had more than one T1-weighted run, we selected the one with the best imaging quality.

Due to the limited samples of female ASD participants, and the consideration that sex-specific developmental trajectories³² and autism-related neuroanatomical differences^{74,75} may confound data-driven population clustering, our study focuses only on male participants under 13 years old. This age range reflects our interest in brain development during childhood and early adolescence. This yielded 274 ASD participants for downstream analyses. The participant ID list is provided in the Supplementary Data 1. Details for participants excluded on each step is provided in Fig. 4.

Pre-processing performed through the self-developed MRI data processing platform: Connectome Computation System (CCS, https://github.com/zuoxinian/CCS) pipeline^{76,77}. CCS optimizes the preprocessing of structural MRI by applying various structure image processing software through script. During our pre-processing, the raw T1-weighted image was first reoriented to RPI orientation and cropped. Skull stripping was then performed using Advanced Normalization Tools (ANTs)⁷⁸ to generate a brain mask. For cortical surface reconstruction and gray and white matter segmentation, the *recon-all* pipeline from FreeSurfer (https://surfer.nmr.mgh.harvard.edu/)(version 6.0.0) was used, with the default brain extraction step replaced by the ANTs-derived brain mask. Each T1-weighted image was segmented into gray matter (GM), white matter (WM), and cerebrospinal fluid (CSF).

The total cortical volume (TCV) was calculated as the sum of the GM and WM volumes, following the LBCC method³². The mean cortical thickness (CT) was calculated as a weighted average of the thicknesses of the left and right hemispheres. The total surface area (SA) was determined by summing the surface areas of white matter of both hemispheres. Regional brain volumes for 34 bilaterally averaged cortical regions were evaluated using Desikan-Killiany parcellation³⁶. To reduce site-related variability, we applied ComBat harmonization⁷⁹. This process was implemented using *neuroCombat* (https://github.com/Jfortin1/ComBatHarmonization) R package.

Normative scoring and clustering analysis

To assess how the brain morphology of each participant aligned with age-standardized normative trajectories, we used the out-of-sample (OoS) centile score³². First, all non-ASD individuals from the site-harmonized ABIDE data set were employed to estimate cohort-specific statistical offsets. The centile scores of each brain measurement were then estimated for all individuals with ASD compared to the offset trajectory (see *Methods: Centile scoring of new MRI data* in the original LBCC work³²). This approach takes advantage of the generalized additive models for location, scale, and shape (GAMLSS)⁸⁰ framework to estimate statistical offsets such as mean, variance, and skewness. These offsets capture individual deviations from typical brain development. OoS scores are comparable between age and cohort. The scoring process was conducted with the publicly available code from Lifespan Charts website (https://github.com/brainchart/Lifespan).

Using OoS scores from 34 brain regions as classification features, we applied spectral clustering⁸¹ among individuals with ASD in the ABIDE cohort. Spectral clustering was selected for its ability to detect nonlinear data structures, which are common in brain imaging datasets. Unlike *k*-means clustering, which relies on centroid-based optimization, spectral clustering

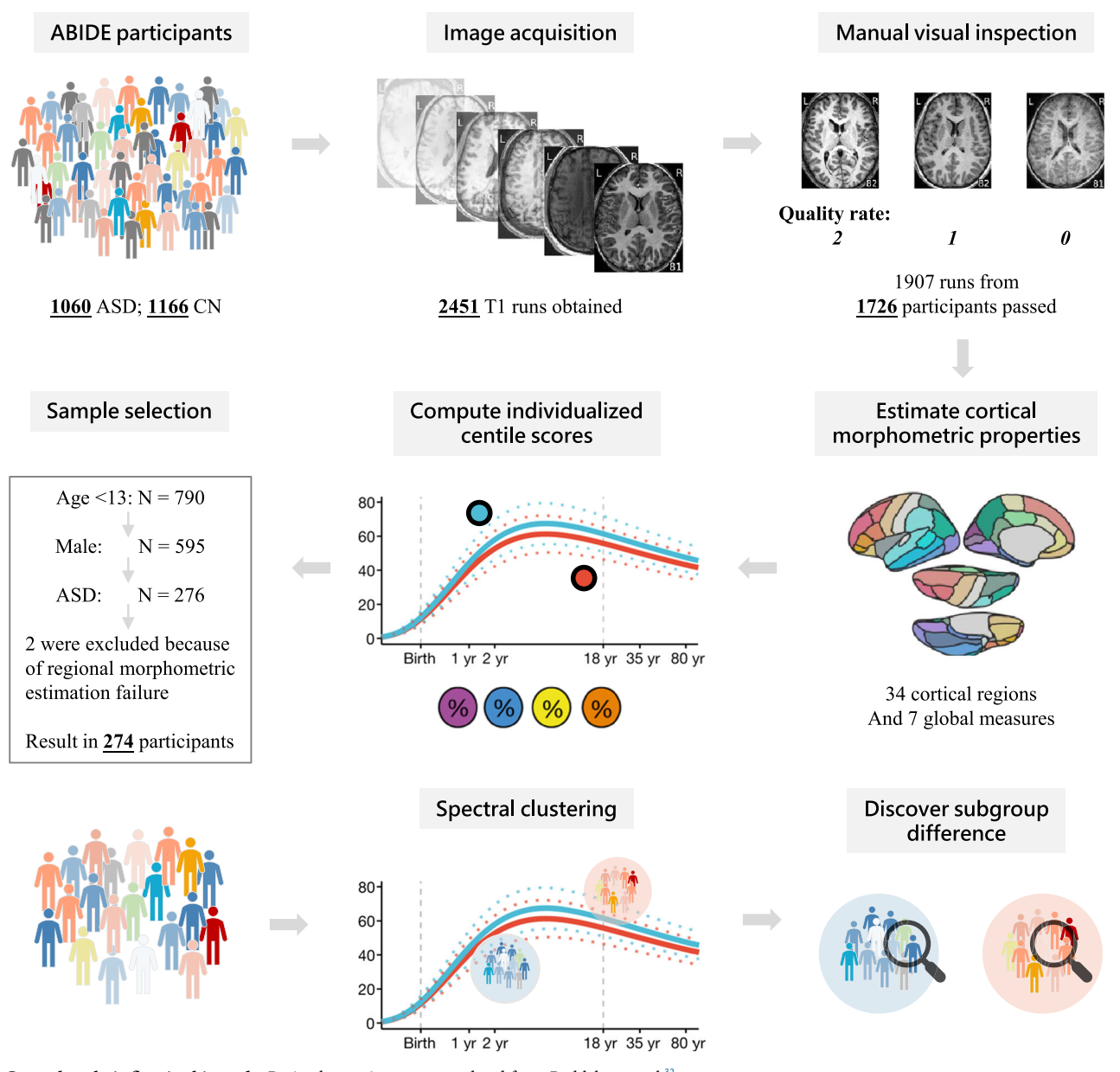


Fig. 4 | General analytic flow in this study. Brain charts pictures are updated from Bethlehem et al. 32.

transforms the data into a lower-dimensional space using the eigenvalues of a similarity matrix. Before clustering, the Jarque-Bera test was performed to determine whether OoS scores follow a normal distribution.

Clustering analysis was implemented using the *kernlab* package R. We tested clusters of 2 to 10 to identify the optimal solution. The quality of clustering was evaluated using the Silhouette Coefficient (SC)⁸², which assesses both within-cluster cohesion and between-cluster separation. SC values range from -1 to 1, with higher scores indicating better defined clusters. The optimal number of clusters was decided by the highest SC score.

Key Brain Regions for Subgroup Classification

We developed a predictive model using machine learning with individual OoS scores from 34 regions of the brain as input characteristics. We trained a Support Vector Machine (SVM) classifier⁸³ with Recursive Feature Elimination and Cross-Validation (RFECV). This was implemented using the *scikit-learn* library in Python. Combining recursive feature elimination (RFE)⁸⁴ with cross-validation allows the model to iteratively identify the most informative features while maintaining generalizability and

robustness. The data set was divided into 80% training sets and 20% testing sets. Using a linear SVM as the base estimator, RFECV removed less important features in a stepwise manner, with performance monitored through 5-fold cross-validation. This process ensured that the final feature set balanced predictive power and reduced over-fitting.

Following feature selection, we fine-tuned the SVM model by performing a grid search to optimize key hyperparameters, including regularization strength (C) and kernel coefficients (γ). The model was evaluated across different kernel functions, such as linear, polynomial, and radial basis functions, to determine the best configuration. Once optimized, the model was trained on the selected features to achieve optimal classification performance. SHapley Additive exPlanations (SHAP)³⁷ were applied to quantify the contribution of each brain region to the model predictions.

Structural covariance network analysis

To investigate morphological relationships of a specific cluster, we constructed structural covariance analysis on OoS scores of each two regions. Pearson's correlation analysis was performed on residuals obtained from linear regression models that controlled for site effects and TCV OoS scores.

To enable statistical comparison, correlation coefficients were normalized using Fisher's *r*-to-*z* transformation, defined as:

$$Z = \frac{1}{2}\log_e\left(\frac{1+r}{1-r}\right),\tag{1}$$

where *r* represents the Pearson correlation coefficient between two regions. The difference (cluster i/ii vs. normal control) in transformed correlation coefficients was calculated using:

$$z = \frac{Z_1 - Z_2}{\sqrt{\frac{1}{n_1 - 3} + \frac{1}{n_2 - 3}}},\tag{2}$$

where n_1 and n_2 are the two sample sizes being compared. The resulting *z*-values were converted to *p*-values using the cumulative distribution function of the standard normal distribution.

Cluster differences and brain-behavior analysis

We investigated differences between clusters and demographic, technical and clinical variables. For categorical variables, such as subtypes of perinatal developmental disorders (PDD), scanner models, and manufacturers, Chisquare tests were employed. For data collection sites, Fisher's exact test was used with Monte Carlo simulations to approximate p values. To ensure robust analysis, sites with fewer than 10 participants were excluded. For other continuous variables, statistical methods were selected based on data distribution: the Wilcoxon rank sum test was used for nonnormally distributed data, and the two-sample t-test for data shows normal distribution. The effect sizes were calculated using Cramér's V for categorical variables and Cohen's d for continuous variables. Statistical significance was set at p < 0.05.

To further explore brain-behavior relationships within clusters, we performed correlation analyses using Full-Scale Intelligence Quotient (FIQ), ADOS-2 (Social Affect and Restricted and Repetitive Behaviors, RRB), ADIR (Social Interaction and RRB), and SRS subscales. Pearson's correlation was applied to most measures, while Spearman's correlation was used for ADOS-2 RRB scores due to their limited range. In these analyzes, the effects of the site and the OoS scores of TCV were controlled. Statistical significance was set at p < 0.05, and no correction for multiple comparisons was applied.

For each group, we also examined partial correlations to investigate structural covariance between 34 brain regions and their association with cognitive behaviors. For each participant, the partial covariance scores of two regions were calculated as:

$$partial_p = residual_{region1} \times residual_{region2}$$
 (3)

The resulting partial covariance scores were then correlated with the same measurements with the same correlated methods.

Finally, we performed mediation analyzes to examine whether FIQ mediates the relationships between brain morphology and cognitive behaviors within clusters. Linear models were used to estimate direct and indirect effects, with adjustments for site and OoS scores of TCV. All brain morphology and cognitive behavior variables were standardized to ensure comparability among participants. The significance of indirect effects was assessed using the Sobel test. As the brain abnormalities are detectable in the early development before the emergence of autistic behaviors. We built a mediation model to examine the brain's effect on cognitive behaviors. To provide a more comprehensive account, we also analyzed the reverse mediation model.

Detection of reproducible results between datasets

We applied the ABIDE-based classifier to an independent dataset from the China Autism Brain Imaging Consortium³³, which is a multicenter collaboration among clinical and research institutions in China. It is designed to collect neuroimaging, demographic, and behavioral data on children and

adolescents with ASD. Diagnoses in the CABIC cohort were based on DSM-IV, DSM-V, or ICD-11 criteria and validated using ADOS and ADI-R. The dataset includes 2,656 participants, including 1,503 ASD individuals and 1,153 typically developing children. Detailed MRI acquisition parameters are publicly accessible at https://php.bdnilab.com/sites/. There were in total 968 ASD males (4.56 \pm 1.69) and 526 (7.37 \pm 2.73) typically controls included into analysis. The participant ID list is provided in the Supplementary Data 2.

CABIC participants, aged 1 to 13 years, tend to exhibit more severe ASD symptoms, resulting in lower variability within clusters. Although this homogeneity is clinically valuable, it poses challenges in detecting subtle brain-behavior relationships. In contrast, the ABIDE cohort provides greater behavioral differences, enhancing the ability to identify nuanced patterns in brain structure. By leveraging these complementary datasets, our goal was to identify results that are reproducible across both cohorts. We repeated the statistical, structural covariance, and correlation analyses on CABIC cohort. However, the limited FIQ data in CABIC restricted the replication of mediation analysis with sufficient statistical power. Therefore, mediation analysis was conducted on the ABIDE cohort only.

In this study, we applied a SVM classifier trained on the ABIDE cohort on the CABIC cohort. To evaluate the consistency between this transfer approach and independent clustering approach, we replicated the identical analytical process directly on ASD participants from CABIC cohort (See details in the Supplementary Information). Optimal cluster solutions was also two (Supplementary Fig. 5a). Among 968 participants, 929 (95.97%) exhibited consistent cluster indices across both methods. This high concordance highlights the robustness of our spectral clustering framework across heterogeneous datasets.

Reporting summary

Further information on research design is available in the Nature Portfolio Reporting Summary linked to this article.

Data availability

The datasets analyzed in this study are publicly available. The ABIDE dataset can be accessed from the Autism Brain Imaging Data Exchange repository at https://fcon_1000.projects.nitrc.org/indi/abide. The CABIC dataset is available upon request through the CABIC Data Sharing Initiative at https://php.bdnilab.com. The key data we used in this study are the OoS centile scores we calculated for each participant with ABIDE and CABIC. To foster researcher on replication and extended exploration, we shared these data through the *Chinese Color Nest Data Community* (https://ccndc.scidb.cn/en) at Science Data Bank in China (https://www.scidb.cn/en/c/o00133). Data have been deposited into CSV files⁸⁷ at https://doi.org/10.57760/sciencedb.24587, and they are accessible upon the requests according to the instructions described on this page.

Code availability

All code used in the analyses is available at https://github.com/XueruFan/ASD-Project. For detailed information on how to use these codes and replicate this study step-by-step, please see the explanation in the READ-ME.md file.

Received: 18 March 2025; Accepted: 21 July 2025; Published online: 05 August 2025

References

- Lord, C., Elsabbagh, M., Baird, G. & Veenstra-Vanderweele, J. Autism spectrum disorder. *Lancet* 392, 508–520 (2018).
- Hirota, T. & King, B. H. Autism spectrum disorder a review. JAMA 329, 157–168 (2023).
- Zeidan, J. et al. Global prevalence of autism: A systematic review update. Autism Res. 15, 778–790 (2022).
- Maenner, M. J. et al. Prevalence and characteristics of autism spectrum disorder among children aged 8 years - autism and

- developmental disabilities monitoring network, 11 Sites, United States, 2020. MMWR Surveill. Summaries 72, 1–14 (2023).
- Zhou, H. et al. Prevalence of autism spectrum disorder in China: A nationwide multi-center population-based study among children aged 6 to 12 years. Neurosci. Bull. 36, 961–971 (2020).
- Fombonne, E. Editorial: The rising prevalence of autism. J. Child Psychol. Psychiatry 59, 717–720 (2018).
- Happé, F. & Frith, U. Annual Research Review: Looking back to look forward – changes in the concept of autism and implications for future research. J. Child Psychol. Psychiatry 61, 218–232 (2020).
- Rabot, J. et al. Genesis, modelling and methodological remedies to autism heterogeneity. Neurosci. Biobehav. Rev. 150 (2023).
- Arvidsson, O., Gillberg, C., Lichtenstein, P. & Lundström, S. Secular changes in the symptom level of clinically diagnosed autism. *J. Child Psychol. Psychiatry* 59, 744–751 (2018).
- van Rooij, D. et al. Cortical and subcortical brain morphometry differences between patients with autism spectrum disorder and healthy individuals across the lifespan: results From the ENIGMA ASD Working Group. Am. J. Psychiatry 175, 359–369 (2018).
- Lombardo, M. V., Lai, M.-C. & Baron-Cohen, S. Big data approaches to decomposing heterogeneity across the autism spectrum. *Mol. Psychiatry* 24, 1435–1450 (2019).
- Marquand, A. F. et al. Conceptualizing mental disorders as deviations from normative functioning. Mol. Psychiatry 24, 1415–1424 (2019).
- Rødgaard, E.-M., Jensen, K., Vergnes, J.-N., Soulières, I. & Mottron, L. Temporal changes in effect sizes of studies comparing individuals with and without autism: a meta-analysis. *JAMA Psychiatry* 76, 1124–1132 (2019).
- Masi, A., DeMayo, M. M., Glozier, N. & Guastella, A. J. An overview of autism spectrum disorder, heterogeneity and treatment options. *Neurosci. Bull.* 33, 183–193 (2017).
- Sandbank, M. et al. Project AIM: Autism intervention meta-analysis for studies of young children. Psychol. Bull. 146, 1–29 (2020).
- Zheng, S., Hume, K. A., Able, H., Bishop, S. L. & Boyd, B. A. Exploring developmental and behavioral heterogeneity among preschoolers with ASD: A cluster analysis on principal components. *Autism Res.* 13, 796–809 (2020).
- Chen, H. et al. Parsing brain structural heterogeneity in males with autism spectrum disorder reveals distinct clinical subtypes. *Hum. Brain Mapp.* 40, 628–637 (2019).
- Shan, X. et al. Mapping the heterogeneous brain structural phenotype of autism spectrum disorder using the normative model. *Biol. Psychiatry* 91, 967–976 (2022).
- Liu, G., Shi, L., Qiu, J. & Lu, W. Two neuroanatomical subtypes of males with autism spectrum disorder revealed using semi-supervised machine learning. *Mol. Autism* 13, 9 (2022).
- Zabihi, M. et al. Fractionating autism based on neuroanatomical normative modeling. *Transl. Psychiatry* 10, 384 (2020).
- Hong, S.-J. et al. Toward neurosubtypes in autism. *Biol. Psychiatry* 88, 111–128 (2020).
- Di Martino, A. et al. Unraveling the miswired Connectome: A developmental perspective. *Neuron* 83, 1335–1353 (2014).
- Russell, G. et al. Selection bias on intellectual ability in autism research: A cross-sectional review and meta-analysis. *Mol. Autism* 10, 9 (2019).
- 24. Feczko, E. et al. The heterogeneity problem: approaches to identify psychiatric subtypes. *Trends Cogn. Sci.* **23**, 584–601 (2019).
- Bedford, S. A. et al. Large-scale analyses of the relationship between sex, age and intelligence quotient heterogeneity and cortical morphometry in autism spectrum disorder. *Mol. Psychiatry* 25, 614–628 (2020).
- Lai, M.-C. et al. Prevalence of co-occurring mental health diagnoses in the autism population: A systematic review and meta-analysis. *Lancet Psychiatry* 6, 819–829 (2019).

- He, Y., Byrge, L. & Kennedy, D. P. Nonreplication of functional connectivity differences in autism spectrum disorder across multiple sites and denoising strategies. *Hum. Brain Mapp.* 41, 1334–1350 (2020).
- Marquand, A. F., Rezek, I., Buitelaar, J. & Beckmann, C. F. Understanding heterogeneity in clinical cohorts using normative models: beyond case-control studies. *Obsess.-Compuls. Disord.* 80, 552–561 (2016).
- Chen, H. et al. Quantile rank maps: A new tool for understanding individual brain development. *NeuroImage* 111, 454–463 (2015).
- Zabihi, M. et al. Dissecting the heterogeneous cortical anatomy of autism spectrum disorder using normative models. *Bridg. Scales: Tech. Transl. Neurosci.* 4, 567–578 (2019).
- Bethlehem, R. A. I. et al. A normative modelling approach reveals ageatypical cortical thickness in a subgroup of males with autism spectrum disorder. Commun. Biol. 3, 486 (2020).
- 32. Bethlehem, R. A. I. et al. Brain charts for the human lifespan. *Nature* **604**, 525–533 (2022).
- Li, L. et al. China Autism Brain Imaging Consortium: Charting brain growth in chinese children with autism. bioRxiv2025.02.20.639044 (2025).
- Di Martino, A. et al. The autism brain imaging data exchange: Towards a large-scale evaluation of the intrinsic brain architecture in autism. Mol. Psychiatry 19, 659–667 (2014).
- Di Martino, A. et al. Enhancing studies of the connectome in autism using the autism brain imaging data exchange II. Sci. Data 4, 170010 (2017).
- Desikan, R. S. et al. An automated labeling system for subdividing the human cerebral cortex on MRI scans into gyral based regions of interest. *NeuroImage* 31, 968–980 (2006).
- Lundberg, S. M. & Lee, S.-I. A unified approach to interpreting model predictions. In *Proceedings of the 31st International Conference on Neural Information Processing Systems*, NIPS'17, 4768-4777 (Curran Associates Inc., Red Hook, NY, USA, 2017).
- Sacco, R., Gabriele, S. & Persico, A. M. Head circumference and brain size in autism spectrum disorder: A systematic review and metaanalysis. *Psychiatry Res.: Neuroimaging* 234, 239–251 (2015).
- 39. Courchesne, E. et al. Mapping early brain development in autism. *Neuron* **56**, 399–413 (2007).
- Bonnet-Brilhault, F. et al. Autism is a prenatal disorder: Evidence from late gestation brain overgrowth. Autism Res. 11, 1635–1642 (2018).
- Courchesne, E. et al. Embryonic origin of two ASD subtypes of social symptom severity: The larger the brain cortical organoid size, the more severe the social symptoms. *Mol. Autism* 15, 22 (2024).
- 42. Courchesne, E. et al. The ASD Living Biology: From cell proliferation to clinical phenotype. *Mol. Psychiatry* **24**, 88–107 (2019).
- Del Casale, A. et al. Neuroanatomical correlates of autism spectrum disorders: A meta-analysis of structural magnetic resonance imaging (MRI) studies. *Psychiatry Res.: Neuroimaging* 325, 111516 (2022).
- Alemany, S., Blok, E., Jansen, P. R., Muetzel, R. L. & White, T. Brain morphology, autistic traits, and polygenic risk for autism: A population-based neuroimaging study. *Autism Res.* 14, 2085–2099 (2021).
- 45. Ashley, S. A. et al. A Longitudinal study of head circumference trajectories in autism and autistic traits. *J. Autism Dev. Disord.* (2024).
- von Rhein, M. et al. Severe congenital heart defects are associated with global reduction of neonatal brain volumes. *J. Pediatr.* 167, 1259–1263.e1 (2015).
- 47. Sigmon, E. R., Kelleman, M., Susi, A., Nylund, C. M. & Oster, M. E. Congenital Heart disease and autism: a case-control study. *Pediatrics* **144**, e20184114 (2019).
- Green, C., Dissanayake, C. & Loesch, D. A review of physical growth in children and adolescents with Autism Spectrum Disorder. *Dev. Rev.* 36, 156–178 (2015).

- Zhao, W. et al. A clustering approach identifies an Autism Spectrum Disorder subtype more responsive to chronic oxytocin treatment. Transl. Psychiatry 14, 312 (2024).
- 50. Rich, S. et al. Patches of disorganization in the neocortex of children with autism. *N. Engl. J. Med.* **370**, 1209–1219 (2014).
- Telencephalon: Neocortex. In Nieuwenhuys, R., Voogd, J. & van Huijzen, C. (eds.) *The Human Central Nervous System*, 491–679 (Springer Berlin Heidelberg, Berlin, Heidelberg, 2008).
- Sepulcre, J., Sabuncu, M. R., Yeo, T. B., Liu, H. & Johnson, K. A. Stepwise connectivity of the modal cortex reveals the multimodal organization of the human brain. *J. Neurosci.* 32, 10649 (2012).
- 53. Sepulcre, J. Functional streams and cortical integration in the human brain. *Neuroscientist* **20**, 499–508 (2014).
- Martínez, K. et al. Sensory-to-cognitive systems integration is associated with clinical severity in autism spectrum disorder. *J. Am. Acad. Child Adolesc. Psychiatry* 59, 422–433 (2020).
- Margulies, D. S. et al. Situating the default-mode network along a principal gradient of macroscale cortical organization. *Proc. Natl Acad. Sci.* 113, 12574–12579 (2016).
- Thomas Yeo, B. T. et al. The organization of the human cerebral cortex estimated by intrinsic functional connectivity. *J. Neurophysiol.* 106, 1125–1165 (2011).
- Du, J. et al. Organization of the human cerebral cortex estimated within individuals: Networks, global topography, and function. *J. Neurophysiol.* 131, 1014–1082 (2024).
- Meyer, A. Paul Flechsig's System of Myelogenetic Cortical Localization in the Light of Recent Research in Neuroanatomy and Neurophysiology Part I. Can. J. Neurol. Sci. 8, 1–6 (1981).
- Schröder, Y. et al. Associations of subclinical autistic-like traits with brain structural variation using diffusion tensor imaging and voxelbased morphometry. *Eur. Psychiatry* 64, e27 (2021).
- Xiao, J. et al. Personalized theta-burst stimulation enhances social skills in young minimally verbal children with autism: A double-blind randomized controlled trial. *Biol. Psychiatry* (2025).
- Dong, H.-M., Margulies, D. S., Zuo, X.-N. & Holmes, A. J. Shifting gradients of macroscale cortical organization mark the transition from childhood to adolescence. *Proc. Natl Acad. Sci.* 118, e2024448118 (2021).
- 62. Warrier, V. et al. Genetic insights into human cortical organization and development through genome-wide analyses of 2,347 neuroimaging phenotypes. *Nat. Genet.* **55**, 1483–1493 (2023).
- Gerlach, C. et al. Brain activity related to integrative processes in visual object recognition: Bottom-up integration and the modulatory influence of stored knowledge. *Neuropsychologia* 40, 1254–1267 (2002).
- Lord, C. et al. A multisite study of the clinical diagnosis of different autism spectrum disorders. Arch. Gen. Psychiatry 69, 306–313 (2012).
- Yoo, S. et al. Whole-brain structural connectome asymmetry in autism. NeuroImage 288 (2024).
- Mottron, L. Progress in autism research requires several recognitiondefinition-investigation cycles. *Autism Res.* 14, 2230–2234 (2021).
- Jack, A. & A. Pelphrey, K. Annual Research Review: Understudied populations within the autism spectrum – current trends and future directions in neuroimaging research. *J. Child Psychol. Psychiatry* 58, 411–435 (2017).
- Figueiredo, M. A. T. & Jain, A. K. Unsupervised learning of finite mixture models. *IEEE Trans. Pattern Anal. Mach. Intell.* 24, 381–396 (2002).
- Constantino, J. N. The quantitative nature of autistic social impairment. *Pediatr. Res.* 69, 55–62 (2011).
- Aglinskas, A., Hartshorne, J. K. & Anzellotti, S. Contrastive machine learning reveals the structure of neuroanatomical variation within autism. *Science* 376, 1070–1074 (2022).

- Veenstra-VanderWeele, J., O'Reilly, K. C., Dennis, M. Y., Uribe-Salazar, J. M. & Amaral, D. G. Translational Neuroscience Approaches to Understanding Autism. *Am. J. Psychiatry* 180, 265–276 (2023).
- Esteban, O. et al. MRIQC: Advancing the automatic prediction of image quality in MRI from unseen sites. *PLOS ONE* 12, e0184661 (2017).
- Rosen, A. F. G. et al. Quantitative assessment of structural image quality. NeuroImage 169, 407–418 (2018).
- Baron-Cohen, S., Knickmeyer, R. C. & Belmonte, M. K. Sex differences in the brain: implications for explaining autism. *Science* 310, 819–823 (2005).
- Bedford, S. A. et al. Brain-charting autism and attention-deficit/ hyperactivity disorder reveals distinct and overlapping neurobiology. *Biol. Psychiatry* 97, 517–530 (2025).
- Xing, X.-X., Xu, T., Jiang, C., Wang, Y.-S. & Zuo, X.-N. Connectome Computation System: 2015–2021 updates. *Sci. Bull.* 67, 448–451 (2022).
- Xu, T., Yang, Z., Jiang, L., Xing, X.-X. & Zuo, X.-N. A Connectome Computation System for discovery science of brain. Sci. Bull. 60, 86–95 (2015).
- Avants, B., Epstein, C., Grossman, M. & Gee, J. Symmetric diffeomorphic image registration with cross-correlation: Evaluating automated labeling of elderly and neurodegenerative brain. Spec. Issue Third Int. Workshop Biomed. Image Registr. – WBIR 2006 12, 26–41 (2008).
- 79. Fortin, J.-P. et al. Harmonization of cortical thickness measurements across scanners and sites. *NeuroImage* **167**, 104–120 (2018).
- 80. Borghi, E. et al. Construction of the World Health Organization child growth standards: Selection of methods for attained growth curves. *Stat. Med.* **25**, 247–265 (2006).
- von Luxburg, U. A tutorial on spectral clustering. Stat. Comput. 17, 395–416 (2007).
- 82. Rousseeuw, P. J. Silhouettes: A graphical aid to the interpretation and validation of cluster analysis. *J. Comput. Appl. Math.* **20**, 53–65 (1987).
- Cortes, C. & Vapnik, V. Support-vector networks. Mach. Learn. 20, 273–297 (1995).
- 84. Guyon, I., Weston, J., Barnhill, S. & Vapnik, V. Gene selection for cancer classification using support vector machines. *Mach. Learn.* **46**, 389–422 (2002).
- Duan, X. et al. Subcortical structural covariance in young children with autism spectrum disorder. *Prog. Neuro-Psychopharmacol. Biol. Psychiatry* 99, 109874 (2020).
- 86. Hazlett, H. C. et al. Early brain development in infants at high risk for autism spectrum disorder. *Nature* **542**, 348–351 (2017).
- 87. Fan, X.-R. & DeepNeuro. Out-of-sample centile scores of brain morphology for participants from ABIDE and CABIC. *Science Data Bank* (2025).

Acknowledgements

The STI 2030 - the major projects of the Brain Science and Brain-Inspired Intelligence Technology (2021ZD0200500), the Key-Area Research and Development Program of Guangdong Province (2019B030335001), the Major Projects of National Social Science Foundation of China (20&ZD296, 24&ZD251), and the National Natural Science Foundation of China (82102134, 82322035, 62273076) provide funding supports.

Author contributions

Conception and Design: X-R.F., X.D., X-N.Z. Data Analysis: X-R.F. MRI Data Preprocessing: Y.H., L.L., Y-S.W., CABIC, LBCC. Initial Drafting of the Manuscript: X-R.F. Critical Review and Editing of the Manuscript: All authors contributed to the critical review and editing of the manuscript.

Competing interests

The authors declare no competing interests.

Additional information

Supplementary information The online version contains supplementary material available at https://doi.org/10.1038/s42003-025-08573-z.

Correspondence and requests for materials should be addressed to Xujun Duan or Xi-Nian Zuo.

Peer review information Communications Biology thanks the anonymous reviewers for their contribution to the peer review of this work. Primary Handling Editor: Jasmine Pan.

Reprints and permissions information is available at http://www.nature.com/reprints

Publisher's note Springer Nature remains neutral with regard to jurisdictional claims in published maps and institutional affiliations.

Open Access This article is licensed under a Creative Commons Attribution-NonCommercial-NoDerivatives 4.0 International License, which permits any non-commercial use, sharing, distribution and reproduction in any medium or format, as long as you give appropriate credit to the original author(s) and the source, provide a link to the Creative Commons licence, and indicate if you modified the licensed material. You do not have permission under this licence to share adapted material derived from this article or parts of it. The images or other third party material in this article are included in the article's Creative Commons licence, unless indicated otherwise in a credit line to the material. If material is not included in the article's Creative Commons licence and your intended use is not permitted by statutory regulation or exceeds the permitted use, you will need to obtain permission directly from the copyright holder. To view a copy of this licence, visit http://creativecommons.org/licenses/by-nc-nd/4 0/

© The Author(s) 2025

Lifespan Brain Chart Consortium (LBCC)

Chris Adamson^{4,5}, Sophie Adler⁶, Aaron F. Alexander-Bloch^{7,8,9}, Evdokia Anagnostou^{10,11}, Kevin M. Anderson¹², Ariosky Areces-Gonzalez^{13,14}, Duncan E. Astle¹⁵, Bonnie Auyeung^{16,17}, Muhammad Ayub^{18,19}, Jong Bin Bae²⁰, Gareth Ball^{4,21}, Simon Baron-Cohen^{17,22}, Richard Beare^{4,5}, Saashi A. Bedford¹⁷, Vivek Benegal²³, Richard A. I. Bethlehem^{17,24}, Frauke Beyer²⁵, John Blangero²⁶, Manuel Blesa Cábez²⁷, James P. Boardman²⁷, Matthew Borzage²⁸, Jorge F. Bosch-Bayard^{29,30}, Niall Bourke^{31,32}, Edward T. Bullmore³³, Vince D. Calhoun³⁴, Mallar M. Chakravarty^{30,35}, Christina Chen³⁶, Casey Chertavian⁹, Gaël Chetelat³⁷, Yap S. Chong^{38,39}, Aiden Corvin⁴⁰, Manuela Costantino^{41,42}, Eric Courchesne^{43,44}, Fabrice Crivello⁴⁵, Vanessa L. Cropley⁴⁶, Jennifer Crosbie⁴⁷, Nicolas Crossley^{48,49}, Marion Delarue³⁷, Richard Delorme^{50,51}, Sylvane Desrivieres⁵², Gabriel Devenyi^{53,54,55}, Maria A. Di Biase^{46,56}, Ray Dolan^{57,58,59}, Kirsten A. Donald^{60,61}, Gary Donohoe⁶², Lena Dorfschmidt^{7,8,9}, Katharine Dunlop⁶³, Anthony D. Edwards^{64,65,66}, Jed T. Elison⁶⁷, Cameron T. Ellis^{12,68}, Jeremy A. Elman⁶⁹, Lisa Eyler^{70,71}, Damien A. Fair⁶⁷, Paul C. Fletcher^{72,73}, Peter Fonagy^{74,75}, Carol E. Franz⁵⁹, Lidice Galan-Garcia⁷⁶, Ali Gholipour⁷⁷, Jay Giedd^{78,79}, John H. Gilmore⁸⁰, David C. Glahn^{81,82}, Ian M. Goodyer³³, P. E. Grant⁸³, Nynke A. Groenewold^{61,84}, Shreya Gudapati^{7,8,9}, Faith M. Gunning⁸⁵, Raquel E. Gur^{7,9}, Ruben C. Gur^{7,86}, Christopher F. Hammill^{47,87}, Oskar Hansson^{88,89}, Trey Hedden^{90,91}, Andreas Heinz⁹², Richard N. Henson^{15,33}, Katja Heuer⁹³, Jacqueline Hoare⁹⁴, Bharath Holla^{95,96}, Avram J. Holmes⁹⁷, Hao Huang⁹⁸, Jonathan Ipser⁹⁹, Clifford R. Jack Jr¹⁰⁰, Andrea P. Jackowski^{101,102}, Tianye Jia^{103,104,105}, David T. Jones^{100,106}, Peter B. Jones^{33,73}, Rene S. Kahn¹⁰⁷. Hasse Karlsson^{108,109}, Linnea Karlsson^{108,109}, Ryuta Kawashima¹¹⁰, Elizabeth A. Kelley¹¹¹, Silke Kern^{112,113}, Ki-Woong Kim^{20,114,115}, Manfred G. Kitzbichler³³, William S. Kremen⁶⁹, François Lalonde¹¹⁶, Brigitte Landeau³⁷, Jason Lerch^{117,118,119}, John D. Lewis¹²⁰, Jiao Li¹²¹, Wei Liao¹²¹, Conor Liston¹²², Michael V. Lombardo^{17,123}, Jinglei Lv^{46,124}, Travis T. Mallard¹²⁵, Machteld Marcelis^{126,127}, Samuel R. Mathias⁸¹, Bernard Mazoyer^{45,128}, Philip McGuire¹²⁹, Michael J. Meaney^{130,131}, Andrea Mechelli¹²⁹, Bratislav Misic¹³², Sarah E. Morgan^{33,133,134}, David Mothersill^{40,135,136}, Cynthia Ortinau¹³⁷, Rik Ossenkoppele^{138,139}, Minhui Ouyang⁹⁸, Lena Palaniyappan¹⁴⁰, Leo Paly³⁷, Pedro M. Pan^{141,142}, Christos Pantelis^{143,144,145}, Min Tae M. Park¹⁴⁶, Tomas Paus^{147,148}, Zdenka Pausova^{47,149}, Deirel Paz-Linares^{13,150}, Alexa Pichet Binette^{151,152}, Karen Pierce¹⁵³, Xing Qian¹⁵⁴, Anqi Qiu¹⁵⁵, Armin Raznahan¹¹⁶, Timothy Rittman¹⁵⁶, Amanda Rodrigue⁸¹, Caitlin K. Rollins^{157,158}, Rafael Romero-Garcia^{33,159}, Lisa Ronan³³, Monica D. Rosenberg¹⁶⁰, David H. Rowitch¹⁶¹, Giovanni A. Salum^{162,163}, Theodore D. Satterthwaite^{7,164}, H. Lina Schaare^{165,166}, Jenna Schabdach^{7,8,9}, Russell J. Schachar⁴⁷, Michael Schöll^{167,168,169}, Aaron P. Schultz^{82,170,171}, Jakob Seidlitz^{7,8,9}, David Sharp^{31,32}, Russell T. Shinohara^{36,172}, Ingmar Skoog^{112,113}, Christopher D. Smyser¹⁷³, Reisa A. Sperling^{82,170,174}, Dan J. Stein¹⁷⁵, Aleks Stolicyn¹⁷⁶, John Suckling^{33,177}, Gemma Sullivan²⁷, Benjamin Thyreau¹¹⁰, Roberto Toro^{93,178}, Nicolas Traut^{179,180}, Kamen A. Tsvetanov^{156,181}, Nicholas B. Turk-Browne^{12,182}, Jetro J. Tuulari^{183,184,185}, Christophe Tzourio¹⁸⁶, Étienne Vachon-Presseau^{187,188,189}, Mitchell J. Valdes-Sosa⁷⁶, Pedro A. Valdes-Sosa^{190,191}, Sofie L. Valk¹⁹², Therese van Amelsvoort¹⁹³, Simon N. Vandekar^{194,195}, Lana Vasung¹⁹⁶, Petra E. Vértes^{33,134}, Lindsay W. Victoria⁸⁵, Sylvia Villeneuve^{151,152,197}, Arno Villringer^{25,198}, Jacob W. Vogel^{7,164}, Konrad Wagstyl¹⁹⁹, Yin-Shan Wang^{1,200,201,202}, Simon K. Warfield⁷⁷, Varun Warrier³³, Eric Westman²⁰³, Margaret L. Westwater³³, Heather C. Whalley^{176,204}, Simon R. White^{33,205}, A. Veronica Witte^{25,198,206}, Ning Yang^{1,200,201,202}, B. T. Thomas Yeo^{207,208,209,210}, Hyuk Jin Yun²¹¹, Andrew Zalesky^{46,212}, Heather J. Zar^{84,213}, Anna Zettergren¹¹², Juan H. Zhou^{154,207,214}, Hisham Ziauddeen^{33,215,216}, Dabriel Zimmerman^{7,8,9}, Andre Zugman^{142,217,218} & Xi-Nian Zuo^{1,200,201,202,219}

⁴Developmental Imaging, Murdoch Children's Research Institute, Melbourne, Vic, Australia. ⁵Department of Medicine, Monash University, Melbourne, Vic, Australia. ⁶UCL Great Ormond Street Institute for Child Health, London WC1N1EH, England. ⁷Department of Psychiatry, University of Pennsylvania, Philadelphia, PA19104, USA. ⁸Department of Child and Adolescent Psychiatry and Behavioral Science, The Children's Hospital of Philadelphia, Philadelphia, PA 19104, USA. ⁹Lifespan Brain Institute, The Children's Hospital of Philadelphia, Philadelphia, PA 19104, USA. 10 Department of Pediatrics University of Toronto, Toronto, Canada. 11 Holland Bloorview Kids Rehabilitation Hospital, Toronto, Canada. 12 Department of Psychology, Yale University, New Haven, CT, USA. 13 The Clinical Hospital of Chengdu Brain Science Institute, MOE Key Lab for NeuroInformation, University of Electronic Science and Technology of China, Chengdu 611731, China. 14 University of Pinar del Río Hermanos Saiz Montes de Oca, Pinar del Río, Cuba. 15 MRC Cognition and Brain Sciences Unit, University of Cambridge, Cambridge, UK. 16 Department of Psychology, School of Philosophy, Psychology and Language Sciences, University of Edinburgh, Edinburgh, UK. 17 Autism Research Centre, Department of Psychiatry, University of Cambridge, Cambridge CB2 0SZ, UK. ¹⁸Queen's University, Department of Psychiatry, Centre for Neuroscience Studies, Kingston, ON, Canada. ¹⁹University College London, Mental Health Neuroscience Research Department, Division of Psychiatry, London, UK. 20 Department of Neuropsychiatry, Seoul National University Bundang Hospital, Seongnam, Korea. 21 Department of Paediatrics, University of Melbourne, Melbourne, Vic, Australia. 22 Cambridge Lifetime Asperger Syndrome Service (CLASS), Cambridgeshire and Peterborough NHS Foundation Trust, Cambridge, UK. 23 Centre for Addiction Medicine, National Institute of Mental Health and Neurosciences (NIMHANS), 560029 Bengaluru, India. 24 Brain Mapping Unit, Department of Psychiatry, University of Cambridge, Cambridge CB2 0SZ, UK. 25 Department of Neurology, Max Planck Institute for Human Cognitive and Brain Sciences, Leipzig 04103, Germany. 26 Department of Human Genetics, South Texas Diabetes and Obesity Institute, University of Texas Rio Grande Valley, Edinburg, USA. 27MRC Centre for Reproductive Health, University of Edinburgh, EdinbCurgh, UK. 28Fetal and Neonatal Institute, Division of Neonatology, Children's Hospital Los Angeles, Department of Pediatrics, Keck School of Medicine, University of Southern California, Los Angeles, CA, USA. 29McGill Centre for Integrative Neuroscience, Ludmer Centre for Neuroinformatics and Mental Health, Montreal Neurological Institute, Montreal, Canada. 30McGill University, Montreal, Canada. 31Department of Brain Sciences, Imperial College London, London, UK. 32Care Research & Technology Centre, UK Dementia Research Institute London, London, UK, 33 Department of Psychiatry, University of Cambridge, Cambridge CB2 9SZ, UK, 34 Tri-institutional Center for Translational Research in Neuroimaging and Data Science, Georgia State University, Georgia Institute of Technology, and Emory University, Atlanta, GA, USA. ³⁵Computational Brain Anatomy (CoBrA) Laboratory, Cerebral Imaging Centre, Douglas Mental Health University Institute, Montreal, Canada. ³⁶Penn Statistics in Imaging and Visualization Center, Department of Biostatistics, Epidemiology, and Informatics, Perelman School of Medicine, University of Pennsylvania, Philadelphia, PA, USA. 37 Normandie Univ, UNICAEN, INSERM, U1237, PhIND "Physiopathology and Imaging of Neurological Disorders", Institut Blood and Brain @ Caen-Normandie, Cyceron, 14000 Caen, France. 38 Singapore Institute for Clinical Sciences, Agency for Science, Technology and Research, Singapore, Singapore. ³⁹Department of Obstetrics and Gynaecology, Yong Loo Lin School of Medicine, National University of Singapore, Singapore, Singapore. ⁴⁰Department of Psychiatry, Trinity College, Dublin, Ireland. 41 Cerebral Imaging Centre, Douglas Mental Health University Institute, Verdun, Canada. 42 Undergraduate program in Neuroscience, McGill University, Montreal, Canada. 43 Department of Neuroscience, University of California, San Diego, San Diego, CA 92093, USA. 44 Autism Center of Excellence, University of California, San Diego, San Diego, CA 92037, USA. 45Institute of Neurodegenerative Disorders, CNRS UMR5293, CEA, University of Bordeaux, Bordeauxm, France. 46 Melbourne Neuropsychiatry Centre, University of Melbourne, Melbourne, Australia. 47 The Hospital for Sick Children, Toronto, Canada. ⁴⁸Department of Psychiatry, School of Medicine, Pontificia Universidad Católica de Chile, Santiago 8330077, Chile. ⁴⁹Department of Psychiatry, University of Oxford, OX3 7JX Oxford, England. 50 Child and Adolescent Psychiatry Department, Robert Debré University Hospital, AP-HP, F-75019 Paris, France. 51 Human Genetics and Cognitive Functions, Institut Pasteur, F-75015 Paris, France. 52 Social, Genetic and Developmental Psychiatry Centre, Institute of Psychiatry, Psychology & Neuroscience, King's College London, London, UK. 53 Cerebral Imaging Centre, Douglas Mental Health University Institute, Montreal, QC, Canada. 54 Department of Psychiatry, McGill University, Montreal, QC, Canada. 55McGill Department of Psychiatry, Montreal, QC, Canada. 56Department of Psychiatry, Brigham and Women's Hospital, Harvard Medical School, Boston, MA, USA. 57 Max Planck UCL Centre for Computational Psychiatry and Ageing Research, University College London, London, UK. 58 Wellcome Centre for Human Neuroimaging, University College London, London, UK. 59 Wellcome Centre for Human Neuroimaging, London WC1N 3AR, UK. 60 Division of Developmental Paediatrics, Department of Paediatrics and Child Health, Red Cross War Memorial Children's Hospital, Klipfontein Road/Private Bag, Rondebosch, 7700/7701 Cape Town, South Africa. 61 Neuroscience Institute, University of Cape Town, Cape Town, South Africa. 62 Center for Neuroimaging, Cognition & Genomics (NICOG), School of Psychology, National University of Ireland Galway, Galway, Ireland. 63 Weil Family Brain and Mind Research Institute, Department of Psychiatry, Weill Cornell Medicine, New York, USA. 64Centre for the Developing Brain, King's College London, London, UK. 65Evelina London Children's Hospital, London, UK. 66MRC Centre for Neurodevelopmental Disorders, London, UK. 67Institute of Child Development, Department of Pediatrics, Masonic Institute for the Developing Brain, University of Minnesota, Minneapolis, MN, USA. 68 Haskins Laboratories, New Haven, CT, USA. 69 Department of Psychiatry, Center for Behavior Genetics of Aging, University of California, San Diego, La Jolla, CA, USA. 70 Desert-Pacific Mental Illness Research Education and Clinical Center, VA San Diego Healthcare, San Diego, CA, USA. 71 Department of Psychiatry, University of California San Diego, Los Angeles, CA, USA. 72 Department of Psychiatry, University of Cambridge, and Wellcome Trust MRC Institute of Metabolic Science, Cambridge Biomedical Campus, Cambridge, UK. 73 Cambridgeshire and Peterborough NHS Foundation Trust, Huntingdon, UK. 74Department of Clinical, Educational and Health Psychology, University College London, London, UK. 75Anna Freud National Centre for Children and Families, London, UK. 76Cuban Center for Neuroscience, La Habana, Cuba. 77Computational Radiology Laboratory, Boston Children's Hospital, Boston, MA 02115, USA. 78 Department of Child and Adolescent Psychiatry, University of California, San Diego, San Diego, CA 92093, USA. 79 Department of Psychiatry, University of California San Diego, San Diego, CA, USA. 80 Department of Psychiatry, University of North Carolina, Chapel Hill, NC, USA. 81 Department of Psychiatry, Boston Children's Hospital and Harvard Medical School, Boston, MA 02115, USA. 82 Harvard Medical School, Boston, MA 02115, USA. 83 Division of Newborn Medicine and Neuroradiology, Fetal Neonatal Neuroimaging and Developmental Science Center, Boston Children's Hospital, Harvard Medical School, Boston, MA 02115, USA. ⁸⁴Department of Paediatrics and Child Health, Red Cross War Memorial Children's Hospital, SA-MRC Unit on Child & Adolescent Health, University of Cape Town, Cape Town, South Africa. 85 Weill Cornell Institute of Geriatric Psychiatry, Department of Psychiatry, Weill Cornell Medicine, New York, USA. 86 Lifespan Brain Institute, The Children's Hospital of Philadelphia, Philadelphia, PA 19105, USA. 87 Mouse Imaging Centre, Toronto, Canada. 88 Clinical Memory Research Unit, Department of Clinical Sciences Malmö, Lund University, Malmö, Sweden. 89 Memory Clinic, Skåne University Hospital, Malmö, Sweden. 90 Department of Neurology, Icahn School of Medicine at Mount Sinai, New York, NY 10029, USA. 91Athinoula A. Martinos Center for Biomedical Imaging, Department of Radiology, Massachusetts General Hospital, Harvard Medical School, Boston, MA 02129, USA. 92 Department of Psychiatry and Psychotherapy, Charite University Hospital Berlin, Berlin, Germany. 93 Institut Pasteur, Université Paris Cité, Unité de Neuroanatomie Appliquée et Théorique, F-75015 Paris, France. 94 Department of Psychiatry, University of Cape Town, Cape Town, South Africa. 95Department of Integrative Medicine, NIMHANS, Bengaluru 560029, India. 96Accelerator Program for Discovery in Brain disorders using Stem cells (ADBS), Department of Psychiatry, NIMHANS, Bengaluru 560029, India. 97 Department of Psychiatry, Brain Health Institute, Rutgers University, Piscataway, NJ, USA. ⁹⁸Department of Radiology, Children's Hospital of Philadelphia and University of Pennsylvania, Philadelphia, PA 19104, USA. ⁹⁹Department of Psychiatry and Mental Health, Clinical Neuroscience Institute, University of Cape Town, Cape Town, South Africa. 100Department of Radiology, Mayo Clinic, Rochester, MN 55905, USA. 101 Department of Psychiatry, Universidade Federal de São Paulo, São Paulo, Brazil. 102 National Institute of Developmental Psychiatry, CNPq, São Paulo, Brazil. 103 Institute of Science and Technology for Brain-Inspired Intelligence, Fudan University, Shanghai 200433, China. 104 Key Laboratory of Computational Neuroscience

and BrainInspired Intelligence (Fudan University), Ministry of Education, Shanghai, China. 105Centre for Population Neuroscience and Precision Medicine (PONS), Institute of Psychiatry, Psychology and Neuroscience, SGDP Centre, King's College London, London SE5 8AF, UK, 106 Department of Neurology, Mayo Clinic, Rochester, MN, USA, 107 Department of Psychiatry, Icahn School of Medicine at Mount Sinai, New York, NY, USA, 108 Department of Clinical Medicine, Department of Psychiatry and Turku Brain and Mind Center, FinnBrain Birth Cohort Study, University of Turku and Turku University Hospital, Turku, Finland. 109 Centre for Population Health Research, Turku University Hospital and University of Turku, Turku, Finland. 110 Institute of Development, Aging and Cancer, Tohoku University, Sendai 980-8575, Japan: 111 Queen's University, Departments of Psychology and Psychiatry, Centre for Neuroscience Studies, Kingston, ON, Canada. 112 Neuropsychiatric Epidemiology Unit, Department of Psychiatry and Neurochemistry, Institute of Neuroscience and Physiology, the Sahlgrenska Academy, Centre for Ageing and Health (AGECAP) at the University of Gothenburg, Gothenburg, Sweden. 113 Region Västra Götaland, Sahlgrenska University Hospital, Psychiatry, Cognition and Old Age Psychiatry Clinic, Gothenburg, Sweden. 114Department of Brain and Cognitive Sciences, Seoul National University College of Natural Sciences, Seoul, Republic of Korea. 115Department of Psychiatry, Seoul National University College of Medicine, Seoul, Republic of Korea. 116 Section on Developmental Neurogenomics, Human Genetics Branch, National Institute of Mental Health, Bethesda, MD, USA. 117 Department of Medical Biophysics, University of Toronto, Toronto, ON, Canada. 118 Mouse Imaging Centre, The Hospital for Sick Children, Toronto, ON, Canada. 119 Wellcome Centre for Integrative Neuroimaging, FMRIB, Nuffield Department of Clinical Neuroscience, University of Oxford, Oxford, UK. 120 Montreal Neurological Institute, McGill University, Montreal, Canada. 121 The Clinical Hospital of Chengdu Brain Science Institute, University of Electronic Science and Technology of China, Chengdu 611731, China. 122 Department of Psychiatry and Brain and Mind Research Institute, Weill Cornell Medicine, New York, USA. 123 Laboratory for Autism and Neurodevelopmental Disorders, Center for Neuroscience and Cognitive Systems @UniTn, Istituto Italiano di Tecnologia, Rovereto, Italy. 124School of Biomedical Engineering & Brain and Mind Centre, The University of Sydney, Sydney, NSW, Australia. 125Department of Psychology, University of Texas, Austin, TX 78712, USA. 126 Department of Psychiatry and Neuropsychology, School of Mental Health and Neuroscience, EURON, Maastricht University Medical Centre, Maastricht, the Netherlands. 128 Bordeaux University Medical Centre, Maastricht, the Netherlands. 128 Bordeaux University Hospital, Bordeaux, France. 129 Professor, Department of Psychosis Studies, Institute of Psychiatry, Psychology and Neuroscience, King's College London, London, UK. 130 Ludmer Centre for Neuroinformatics and Mental Health, Douglas Mental Health University Institute, McGill University, Montreal, QC, Canada. 131 Singapore Institute for Clinical Sciences, Singapore, Singapore. 132 McConnell Brain Imaging Centre, Montreal Neurological Institute, McGill University, Montreal, QC H3A 2B4, Canada. 133Department of Computer Science and Technology, University of Cambridge, Cambridge, UK. 134The Alan Turing Institute, London NW1 2DB, UK. 135Department of Psychology, School of Business, National College of Ireland, Dublin, Ireland. 136School of Psychology & Center for Neuroimaging and Cognitive Genomics, National University of Ireland Galway, Galway, Ireland. 137 Department of Pediatrics, Washington University in St. Louis, St. Louis, MI, USA. 138 Alzheimer Center Amsterdam, Department of Neurology, Amsterdam Neuroscience, Vrije Universiteit Amsterdam, Amsterdam UMC, Amsterdam, The Netherlands. 139Lund University, Clinical Memory Research Unit, Lund, Sweden. 140 Robarts Research Institute & The Brain and Mind Institute, University of Western Ontario, London, ON, Canada. 141 Department of Psychiatry, Federal University of Sao Poalo (UNIFESP), Sao Poalo, Brazil. 142 National Institute of Developmental Psychiatry for Children and Adolescents (INPD), Sao Poalo, Brazil. 143 Melbourne Neuropsychiatry Centre, Department of Psychiatry, The University of Melbourne and Melbourne Health, Carlton South, Vic, Australia. 144 Melbourne School of Engineering, The University of Melbourne, Parkville, Vic, Australia. 145 Florey Institute of Neuroscience and Mental Health, Parkville, VIC, Australia. 146 Department of Psychiatry, Schulich School of Medicine and Dentistry, Western University, London, ON, Canada. 147 Department of Psychiatry, Faculty of Medicine and Centre Hospitalier Universitaire Sainte-Justine, University of Montreal, Montreal, QC, Canada. 148 Departments of Psychiatry and Psychology, University of Toronto, Toronto, ON, Canada. 149 Departments of Physiology and Nutritional Sciences, University of Toronto, Toronto, Canada. 150 Cuban Neuroscience Center, Havana, Cuba. 151 Department of Psychiatry, Faculty of Medicine, McGill University, Montreal, QC H3A 1Y2, Canada. 152 Douglas Mental Health University Institute, Montreal, QC H4H 1R3, Canada. 153 Department of Neurosciences, University of California, San Diego La Jolla, CA, USA. 154 Center for Sleep and Cognition, Yong Loo Lin School of Medicine, National University of Singapore, Singapore, Singapore. 155 Department of Biomedical Engineering, The N.1 Institute for Health, National University of Singapore, Singapore, Singapore. ¹⁵⁶Department of Clinical Neurosciences, University of Cambridge, Cambridge, UK. ¹⁵⁷Department of Neurology, Harvard Medical School, Boston, USA. 158 Department of Neurology, Boston Children's Hospital, Boston, MA 02115, USA. 159 Instituto de Biomedicina de Sevilla (IBIS) HUVR/CSIC/Universidad de Sevilla, Dpto. de Fisiología Médica y Biofísica, Seville, Spain. 160 Department of Psychology, Neuroscience Institute, University of Chicago, Chicago, USA. 161 Department of Paediatrics and Wellcome-MRC Cambridge Stem Cell Institute, University of Cambridge, Cambridge, UK. 162 Department of Psychiatry, Universidade Federal do Rio Grande do Sul (UFRGS), Porto Alegre, Brazil. 163 National Institute of Developmental Psychiatry (INPD), Sao Poalo, Brazil. 164 Lifespan Informatics & Neuroimaging Center, University of Pennsylvania, Philadelphia, PA 19104, USA. 165 Otto Hahn Group Cognitive Neurogenetics, Max Planck Institute for Human Cognitive and Brain Sciences, Leipzig, Germany. 166 Institute of Neuroscience and Medicine (INM-7: Brain and Behaviour), Research Centre Juelich, Juelich, Germany. 167 Wallenberg Centre for Molecular and Translational Medicine, University of Gothenburg, Gothenburg, Sweden. 168 Department of Psychiatry and Neurochemistry, University of Gothenburg, Gothenburg, Sweden. 169Dementia Research Centre, Queen's Square Institute of Neurology, University College London, London, UK. 170 Harvard Aging Brain Study, Department of Neurology, Massachusetts General Hospital, Boston, MA 02114, USA. 171 Athinoula A. Martinos Center for Biomedical Imaging, Department of Radiology, Massachusetts General Hospital, Charlestown, MA 02129, USA. 172Center for Biomedical Image Computing and Analytics, Department of Radiology, Perelman School of Medicine, University of Pennsylvania, Philadelphia, PA, USA. 173 Departments of Neurology, Pediatrics, and Radiology, Washington University School of Medicine, St. Louis, USA. 174Center for Alzheimer Research and Treatment, Department of Neurology, Brigham and Women's Hospital, Boston, MA 02115, USA. 175SA MRC Unit on Risk & Resilience in Mental Disorders, Dept of Psychiatry and Neuroscience Institute, University of Cape Town, Cape Town, South Africa. 176 Division of Psychiatry, Centre for Clinical Brain Sciences, University of Edinburgh, Edinburgh, UK. 177 Cambridge and Peterborough Foundation NHS Trust, Fulbourn, England. 178 Université de Paris, Paris, France. 179 Department of Neuroscience, Institut Pasteur, Paris, France. 180 Center for Research and Interdisciplinarity (CRI), Université Paris Descartes, Paris, France. 181 Department of Psychology, University of Cambridge, Cambridge, UK. 182 Wu Tsai Institute, Yale University, New Haven, CT, USA. 183 Department of Clinical Medicine, Department of Psychiatry, FinnBrain Birth Cohort Study, University of Turku, Turku, Finland. 184 Department of Clinical Medicine, University of Turku, Turku, Finland. 185 Turku Collegium for Science, Medicine and Technology, University of Turku, Turku, Finland. 186 Univ. Bordeaux, Inserm, Bordeaux Population Health Research Center, U1219, Bordeaux, France. 187 Faculty of Dental Medicine and Oral Health Sciences, McGill University, Montreal, QC, Canada. 188 Faculty of Dentistry, McGill University, Montreal, QC, Canada. 189 Alan Edwards Centre for Research on Pain (AECRP), McGill University, Montreal, QC, Canada. 190 Joint China-Cuba Lab, University of Electronic Science and Technology, Chengdu China/Cuban Center for Neuroscience, La Habana, Cuba. 191 University of Electronic Science and Technology of China/Cuban Center for Neuroscience, Chengdu, China. 192 Institute for Neuroscience and Medicine 7, Forschungszentrum Juelich; Max Planck Institute for Human Cognitive and Brain Sciences, Leipzig, Germany. 193 Department of Psychiatry & Neurosychology, Maastricht University, Maastricht, The Netherlands. 194 Department of Biostatistics, Vanderbilt University, Nashville, TN, USA. 195 Department of Biostatistics, Vanderbilt University Medical Center, Nashville, TN, USA. 196Division of Newborn Medicine, Fetal Neonatal Neuroimaging and Developmental Science Center, Department of Pediatrics, Boston Children's Hospital, Boston, MA, USA. 197McConnell Brain Imaging Center, Montreal Neurological Institute, McGill University, Montreal, QC, Canada. 198 Clinic for Cognitive Neurology, University of Leipzig Medical Center, Leipzig, Germany. 199 Wellcome Centre for Human Neuroimaging, Institute of Neurology, University College London, London, England. 200 Developmental Population Neuroscience Research Center, IDG/McGovern Institute for Brain Research, Beijing Normal University, Beijing, China. 201 National Basic Science Data Center, Beijing, China. 202 Research Center for Lifespan Development of Brain and Mind, Institute of Psychology, Chinese Academy of Sciences, Beijing 100101, China. ²⁰³Division of Clinical Geriatrics, Center for Alzheimer Research, Department of Neurobiology, Care Sciences and Society, Karolinska Institutet, Stockholm, Sweden. ²⁰⁴Generation Scotland, University of Edinburgh, Edinburgh, Scotland. ²⁰⁵MRC Biostatistics Unit, University of Cambridge, Cambridge, England. ²⁰⁶Faculty of Medicine, CRC 1052 - Obesity Mechanisms', University of Leipzig, Leipzig, Germany. ²⁰⁷Department of Electrical and Computer Engineering, National University of Singapore, Singapore, Singapore. ²⁰⁸Centre for Sleep & Cognition and Centre for Translational MR Research, Yong Loo Lin School of Medicine, National University of Singapore, Singapore, Singapore. ²⁰⁹N.1 Institute for Health & Institute for Digital Medicine, National University of Singapore, One Department of Biomedical Engineering, University of Melbourne, Melbourne, Australia. ²¹³SAMRC Unit on Child & Adolescent Health, University of Cape Town, Cape Town, South Africa. ²¹⁴Center for Translational Magnetic Resonance Research, Yong Loo Lin School of Medicine, National University of Singapore, Singapor

China Autism Brain Imaging Consortium (CABIC)

Miaoshui Bai²²⁰, Jinhua Cai²²¹, Kelong Cai^{222,223}, Doudou Cao²²⁴, Xuan Cao²²⁵, Aiguo Chen^{223,226}, Huafu Chen²²⁷, Jie Chen²²⁸, Xujun Duan²²⁷, Xue-Ru Fan²²⁹, Peng Gao²²⁹, Wenjing Gao^{230,231}, DongZhi He²³⁰, Feiyong Jia²²⁰, Haoxiang Jiang²³², Xi Jiang²²⁰, Jin Jing²³³, Lei Li²²⁷, Shijun Li²²⁴, Tingyu Li²²⁸, Xiuhong Li²³⁴, Lizi Lin²³³, Yingqiang Liu²²⁷, Zhimei Liu²³⁵, Fanchao Meng^{236,237}, Litong Ni²²⁴, Ning Pan²³⁸, Qi Qi²²⁴, Bin Qin²²¹, Xiaolong Shan²²⁷, Xiaojing Shou^{229,236,239}, Jia Wang²²⁵, Longlun Wang²²¹, Miaoyan Wang²³², Wei Wang²⁴⁰, Xin Wang²³⁸, Lijie Wu²²⁵, Dandan Xu²³², Yin Xu²²⁸, Yang Xue²²⁰, Ting Yang²²⁸, Xuntao Yin²³⁰, Rong Zhang^{236,239}, Yun Zhang²²¹ & Xi-Nian Zuo²²⁹

²²⁰Department of developmental and behavioral pediatrics, Children's Medical Center, The First Hospital of Jilin University, Jilin university, Changchun 130021, China. ²²¹Department of Radiology, Children's Hospital of Chongqing Medical University, Chongqing 400042, China. ²²²College of Physical Education, Yangzhou University, Yangzhou 225127, China, 223 School of Sport and Brain Health, Naniing Sport Institute, Naniing 210014, China, 224 Department of Radiology, First Medical Center, Chinese PLA General Hospital, Beijing 100853, China. 225 Department of Children's and Adolescent Health, Public Health College of Harbin Medical University, Harbin 150086, China. 226 Naniing Sport Institute, Naniing 210014, China. 227 The Clinical Hospital of Chengdu Brain Science Institute, School of Life Science and Technology. University of Electronic Science and Technology of China, Chengdu 610054, China. 228 Children's Nutrition Research Center, Ministry of Education Key Laboratory of Child Development and Disorders, National Clinical Research Center for Child Health and Disorders, China International Science and Technology Cooperation Base of Child Development and Critical Disorders, Children's Hospital of Chongqing Medical University, Chongqing 400042, China. 229 State Key Laboratory of Cognitive Neuroscience and Learning, Developmental Population Neuroscience Research Center at IDG/McGovern Institute for Brain Research, Beijing Normal University, Beijing 100875, China. 230 Department of Radiology, Guangzhou Women and Children's Medical Center, Guangzhou Medical University, Guangzhou 511400, China. 231 School of Public Health, Shenzhen, Sun Yat-sen University, Shenzhen, China. 232 Department of Radiology, Affiliated Children's Hospital of Jiangnan University, Wuxi 214000, China. 233 Department of Maternal and Child Health, Joint International Research Laboratory of Environment and Health, Ministry of Education, Guangdong Provincial Engineering Technology Research Center of Environmental Pollution and Health Risk Assessment, School of Public Health, Sun Yat-sen University, Guangzhou 510080, China. 234Department of Maternal and Child Health and Aging Health, School of Public Health, Shenzhen, Sun Yat-sen University, Shenzhen, China. 235Department of Rehabilitation Medicine, Affiliated Hospital of Yangzhou University, Yangzhou 225001, China. 236 Department of Neurobiology, School of Basic Medical Sciences, Peking University Health Science Center, Beijing 100191, China. 237The National Clinical Research Center for Mental Disorders & Beijing Key Laboratory of Mental Disorders, Beijing Anding Hospital, Capital Medical University, Beijing, China. 238 Key Laboratory of Brain, Cognition and Education Sciences, Ministry of Education, Institute for Brain Research and Rehabilitation, Guangdong Key Laboratory of Mental Health and Cognitive Science, South China Normal University, Guangzhou 510630, China. 239 Key Laboratory for Neuroscience, Ministry of Education / National Health Commission, Peking University, Beijing 100191, China. 240 Department of Radiology, Affiliated Hospital of Yangzhou University, Yangzhou 225001, China.